Received: 22 March 2017 | Revised: 15 July 2017 | Accepted: 4 August 2017

DOI: 10.1002/rnc.3921

RESEARCH ARTICLE

WILEY

Formations on directed cycles with bearing-only measurements

Minh Hoang Trinh[1] | Dwaipayan Mukherjee[2] | Daniel Zelazo[2] | Hyo-Sung Ahn[1]

[1]School of Mechanical Engineering, Gwangju Institute of Science and Technology, Gwangju, South Korea

[2]Faculty of Aerospace Engineering, Technion-Israel Institute of Technology, Haifa, Israel

Correspondence
Hyo-Sung Ahn, School of Mechanical Engineering, Gwangju Institute of Science and Technology, Gwangju 500-712, South Korea.
Email: hyosung@gist.ac.kr

Funding information
National Research Foundation of Korea, Grant/Award Number: NRF-2017R1A2B3007034; Israel Council for Higher Education; Israel Science Foundation, Grant/Award Number: 1490/1

Summary

This paper studies a bearing-only–based formation control problem for a group of single-integrator agents with directed cycle sensing topology. In a 2-dimensional space, a necessary and sufficient condition for the set of desired bearing vectors to be feasible is derived. Then, we propose a bearing-only control law for every agent and prove that the formation asymptotically converges to a formation specified by a set of feasible desired bearing vectors. Analysis of the equilibrium formations in the plane for a 3-agent system and subsequent extension to an n-agent system is provided. We further extend the analysis on directed triangular formation into a 3-dimensional space. Finally, simulations validate the theoretical results.

KEYWORDS

bearing-only measurements, cycle digraph, formation control

1 | INTRODUCTION

Formation control is a widely studied topic in the domain of multiagent systems.[1-5] Based on the sensed and controlled variables, Oh et al[6] classified formation control problems into position-based, displacement-based, distance-based, and bearing-based setups. Recently, as vision sensors and vision-based techniques are becoming ubiquitous, bearing-based formation control has generated a lot of research interest.[7-10]

In bearing-based formation control problems, a group of autonomous agents is required to achieve a target formation shape defined by some bearing variables. These variables are known as the subtended bearing angles or the relative bearing vectors.[11] In previous works,[7,8,12] formation stabilization control laws, using only the bearing angles, were proposed for 3- and 4-agent systems. In the work of Zhao et al,[13] an n-agent formation with an undirected cycle graph was investigated by controlling the subtended bearings. Since the target formation defined by n subtended bearing angles is nonunique, the stability of the equilibrium formation holds only in a local sense.[13] A sufficient condition for the uniqueness of a formation configuration, defined by the bearing vectors, was studied in the work of Zhao and Zelazo.[14] It was shown that a formation shape is unique if it is *infinitesimal bearing rigid*. Furthermore, Zhao and Zelazo[14] also proposed a bearing-only control law that almost globally stabilizes any infinitesimally bearing rigid equilibrium formation. Bearing rigidity theories in SE(2) and SE(3) are recently proposed in the works of Zelazo et al,[15] Schiano et al,[16] and Michieletto et al.[17] Strategies for formation control and estimation were also proposed in the works of Zelazo et al[15] and Schiano et al,[16] assuming that agents can exchange their local sensing information and computations.

While bearing-only formation control problem with undirected sensing graphs has been studied in some detail,[9,14] results on bearing-only formation control with directed sensing graphs are rare. In previous works,[18-20] the leader-first

follower formation has been studied using the notion of input-to-state stability. In the works of Zhao and Zelazo,[21,22] a directed topology was considered and sufficient conditions for the stability of the formations were derived. However, relative position information was also used therein. In fact, investigation of stable bearing-only formation control over a general directed sensing topology is still an open problem.

This paper mainly focuses on a bearing-only formation control problem with a directed cycle sensing graph. More specifically, the n-agent formation in the plane and a 3-agent formation in the 3-dimensional space with directed cycles sensing graphs are studied. First, we derive necessary and sufficient conditions for planar formation feasibility in terms of some algebraic constraints on the set of desired bearing vectors. Second, we propose a bearing-only control law, for agents in cyclic pursuit, to achieve some desired formation and examine the possible equilibrium formations under this law. By classifying these equilibria into the set of desired equilibria and the set of undesired ones, local properties of the equilibria in each set are investigated. Third, by transforming the dynamics of the agents from the position variables to the angular errors, we prove local asymptotic stability of the desired equilibrium and provide an estimate of the corresponding region of attraction. The 3-agent formation is studied in detail since its sensing graph is the only one in this class satisfying the infinitesimal rigidity condition. The analysis of the $n-$agent case is then given as a natural extension of the 3-agent scenario. Finally, we extend the analysis on directed triangular formations to 3 dimensions. Although formations of directed cycles with more than 3 agents in $\mathbb{R}^2$ are not bearing rigid, studying directed cycles may aid in a better understanding of stabilizing formations with general digraphs. Another motivation comes from hardware implementability of the formation, where each agent has a limited vision-based sensing capability. Suppose we have a system of drones and each drone is equipped with a camera-based vision system. To obtain the bearing vector, each drone must detect its neighboring agents based on the image obtained from the camera. Since the detecting task may be challenging because of environmental noises and obstacles, it is desired to limit the number of neighbors that needs to be kept track of in the sensing graph. The directed cycle is a strongly connected graph with the least number of edges and is thus easier to implement on hardware. Note that a related study of bearing-only cyclic pursuit for target capture can be found in our previous works.[23,24] In the aforementioned works,[23,24] under the assumption that all agents in cyclic pursuit can also sense the bearing with respect to a stationary target, the formation shape is uniquely determined up to a scaling factor. However, we[23,24] presented no analysis on asymptotic stability of these formations. The problem considered in this paper is related to cyclic pursuit[25-30] (in which the interaction topology is also described by a cycle graph) and bearing-only localization problems.[31-33] However, this paper attempts to study a bearing-only–based formation control problem with directed cycle sensing graphs. To the best of our knowledge, this problem has not been studied in the existing literature. Furthermore, the necessary and sufficient condition for formation feasibility, discussed in this work, is novel. Finally, our analysis on directed triangular formations in the 3-dimensional space is also a new contribution since almost all previous works mostly focus on 2-dimensional setups.

The remainder of this paper is organized in the following manner. In Section 2, some preliminary results on bearing-only formation are described and the main problem is formulated. Section 3 presents the main stability results pertaining to bearing-only formation control using cyclic pursuit in the plane. Section 4 extends the analysis of directed triangular formations to the 3-dimensional space. In Section 5, simulations validate the theoretical developments. Finally, Section 6 concludes this paper and outlines directions for future investigations.

2 | PROBLEM FORMULATION AND THE PROPOSED CONTROL LAW

2.1 | Problem formulation

Consider a formation of n ($n \geq 3$) autonomous agents in $\mathbb{R}^d$ ($d = 2$ or 3 and will be clear from the context). The dynamics of each agent is given by a single-integrator model

$$\dot{\mathbf{p}}_i = \mathbf{u}_i, \forall i = 1, \ldots, n, \tag{1}$$

where $\mathbf{p}_i$ and $\mathbf{u}_i \in \mathbb{R}^d$ are the position and the control inputs of agent i expressed in the global coordinate frame, respectively.

We use directed graphs to describe the sensing and controlling topology between agents in the formation.[29,34] A directed graph is described by $\mathcal{G} = (\mathcal{V}, \mathcal{E})$, where $\mathcal{V} = \{1, \ldots, n\}$ is the set of nodes and $\mathcal{E} = \{(i,j)|i,j \in \mathcal{V}\}$ is the set of directed edges. A node j is called a neighbor of node i if and only if $(i,j) \in \mathcal{E}$. Let $\mathcal{N}_i$ denote the set of neighbor nodes of i. A *directed cycle* with n nodes (and n edges), denoted by $\mathcal{C}_n$, is a directed graph, where node $i+1$ (modulo n) is the only neighbor of

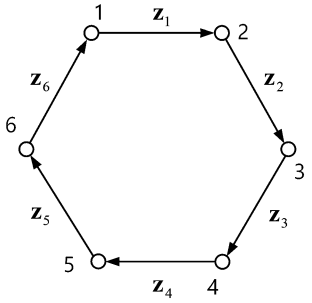

FIGURE 1 A directed cycle graph with 6 nodes

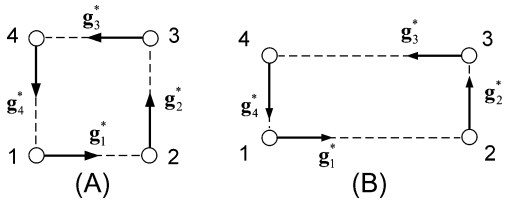

FIGURE 2 Both configurations A, and B, satisfy all desired bearing vectors $\mathbf{g}_i^*, i = 1, \ldots, 4$, but are not similar

node i, ie, $\mathcal{N}_i = \{i + 1(\text{modulo } n)\}$. A directed cycle of 6 nodes is illustrated in Figure 1. We define the relative position vector as $\mathbf{z}_i = \mathbf{p}_{i+1} - \mathbf{p}_i$, for $i = 1, \ldots, n$. The variable $\mathbf{z}_i$ is sometimes referred to as the edge $(i, i + 1)$ in the Euclidean space. Furthermore, $d_i = \|\mathbf{z}_i\|$ is the distance between the 2 agents i and $i + 1$. In addition, let the absolute and relative positions be stacked as vectors $\mathbf{p} = \left[\mathbf{p}_1^T, \ldots, \mathbf{p}_n^T\right]^T \in \mathbb{R}^{dn}$ and $\mathbf{z} = \left[\mathbf{z}_1^T, \ldots, \mathbf{z}_n^T\right]^T \in \mathbb{R}^{dn}$, respectively.

Assume that agent i can measure the bearing with respect to agent $i+1$ (modulo n). Based on the bearing measurement, agent i can obtain the relative bearing vector[35]

$$\mathbf{g}_i = \frac{\mathbf{p}_{i+1} - \mathbf{p}_i}{\|\mathbf{p}_{i+1} - \mathbf{p}_i\|} = \frac{\mathbf{z}_i}{\|\mathbf{z}_i\|}. \tag{2}$$

The unit vector $\mathbf{g}_i$ contains the direction information from agent i to agent $i + 1$. Suppose agent i also knows a desired bearing vector $\mathbf{g}_i^*$ and the control objective is to asymptotically reduce the bearing error between $\mathbf{g}_i$ and $\mathbf{g}_i^*$ to zero. The following definition describes admissible desired bearings.

Definition 1. The set $\mathcal{B}_n = \{\mathbf{g}_i^*\}_{i\in\mathcal{V}}$ is called a *feasible bearing vector set* if and only if, for each $i \in \mathcal{V}$, $\mathbf{g}_i^* \neq \pm\mathbf{g}_{i+1}^*$ and there exist strictly positive scalars d_i such that $\sum_{i=1}^n d_i\mathbf{g}_i^* = \mathbf{0}$.

It follows from Definition 1 that, when the desired bearing vectors belong to set $\mathcal{B}_n$, there do not exist 3 consecutive agents $i - 1, i$ and $i + 1$ whose desired positions are collinear. The condition $\sum_{i=1}^n d_i\mathbf{g}_i^* = \mathbf{0}$ implies that the desired formation of the agents is a closed polygon because each vector of the form $d_i\mathbf{g}_i^*$ is essentially an edge of the desired polygon, connecting agents i and $i + 1$, with $\mathbf{g}_i^*$ being the desired bearing of agent i with respect to its leader, ie, agent $i + 1$. The scalar d_i is the length of the edge between agents i and $i + 1$ and is thus the distance between agents i and $i + 1$ in the Euclidean space corresponding to a feasible formation.

For $n = 3$, every triangular formation satisfying a given desired bearing configuration in $\mathcal{B}_3$ is related by translations and a dilation to another feasible formation. For $n > 3$, this property is generally not true. To see this, consider a 4-agent formation, as shown in Figure 2, which depicts 2 configurations in $\mathbb{R}^2$ with sensing graph $\mathcal{C}_4$. The desired bearing vectors are given by $\mathbf{g}_1^* = [1, 0]^T, \mathbf{g}_2^* = [0, 1]^T, \mathbf{g}_3^* = [-1, 0]^T$, and $\mathbf{g}_4^* = [0, -1]^T$. Although both Figures 2A and 2B satisfy the desired bearings, the formation shapes are not similar. Similarity between formations can only be achieved if the *infinitesimal bearing rigidity* conditions in the work of Zhao and Zelazo[14] are satisfied. However, for $n > 3$, such conditions do not hold for a cycle digraph, so the formation shape is not fixed for a given set of desired bearing vectors.

In $\mathbb{R}^2$, we define $\mathbf{g}_i^\perp = \mathbf{J}\mathbf{g}_i = \begin{bmatrix} 0 & -1 \\ 1 & 0 \end{bmatrix} \mathbf{g}_i$ as the unit vector perpendicular to $\mathbf{g}_i$ in the counterclockwise direction. Note that $\mathbf{J}^T = -\mathbf{J}$. The following result characterizes a condition for feasibility of a set $\mathcal{B}_n$ in $\mathbb{R}^2$.

Lemma 1. *In $\mathbb{R}^2$, the set $\mathcal{B}_n$ is a feasible bearing vector set if and only if, for all $i \in \mathcal{V}$, $\mathbf{g}_i^* \neq \pm\mathbf{g}_{i+1}^*$, and there exist $j, k \in \mathcal{V}\backslash\{i\}$ such that $(\mathbf{g}_j^*)^T\mathbf{g}_i^{*\perp} < 0$ and $(\mathbf{g}_k^*)^T\mathbf{g}_i^{*\perp} > 0$.*

Proof. (*Necessity*) Suppose $\mathcal{B}_n$ is a feasible bearing vector set. There exist positive scalars d_i such that

$$\sum_{i=1}^{n} d_i \mathbf{g}_i^* = \mathbf{0}. \tag{3}$$

We shall prove that there exist $j, k \in \mathcal{V}\backslash\{i\}$ such that $(\mathbf{g}_j^*)^T \mathbf{g}_i^{*\perp} < 0$ and $(\mathbf{g}_k^*)^T \mathbf{g}_i^{*\perp} > 0$ by contradiction.

Suppose there does not exist any $j \in \mathcal{V}\backslash\{i\}$ such that $(\mathbf{g}_j^*)^T \mathbf{g}_i^{*\perp} < 0$. Then, rewriting Equation 3 as

$$-\frac{1}{d_i} \sum_{l\neq i, l=1}^{n} d_l \mathbf{g}_l^* = \mathbf{g}_i^* \tag{4}$$

and premultiplying both sides of Equation 4 with $(\mathbf{g}_i^{*\perp})^T$, we have

$$-\frac{1}{d_i} \sum_{l\neq i, l=1}^{n} d_l \left(\mathbf{g}_i^{*\perp}\right)^T \mathbf{g}_l^* = \left(\mathbf{g}_i^{*\perp}\right)^T \mathbf{g}_i^* = 0. \tag{5}$$

Since $(\mathbf{g}_i^{*\perp})^T \mathbf{g}_l^* \geq 0$, for all $l \neq i$, the left-hand side of Equation 5 is nonpositive. In fact, since $\mathbf{g}_{i+1}^* \neq \pm \mathbf{g}_i^*$, we have $(\mathbf{g}_i^{*\perp})^T \mathbf{g}_{i+1}^* \neq 0$, which implies that the left-hand side of Equation 5 is negative. However, the right-hand side of Equation 5 is zero. This contradiction implies that there exists at least one $j \in \mathcal{V}\backslash\{i\}$ such that $(\mathbf{g}_j^*)^T \mathbf{g}_i^{*\perp} < 0$. Similarly, the existence of at least some $k \in \mathcal{V}\backslash\{i\}$ such that $(\mathbf{g}_k^*)^T \mathbf{g}_i^{*\perp} > 0$ is also necessary for a feasible bearing set.

(*Sufficiency*) Suppose that, for all $i \in \mathcal{V}$, $\mathbf{g}_i^* \neq \pm \mathbf{g}_{i+1}^*$, and there are $j, k \in \mathcal{V}\backslash\{i\}$ such that $(\mathbf{g}_j^*)^T \mathbf{g}_i^{*\perp} < 0$ and $(\mathbf{g}_k^*)^T \mathbf{g}_i^{*\perp} > 0$. We shall prove that there exist positive scalars d_i such that Equation 3 is satisfied. The proof contains the following steps.

Step 1: If $\mathbf{g}_k^* \neq -\mathbf{g}_j^*$, we go to Step 2. Otherwise, if $\mathbf{g}_k^* = -\mathbf{g}_j^*$, we shall show that there exists $l \in \mathcal{V}\backslash\{i, j, k\}$ such that $\mathbf{g}_l^* \neq \pm \mathbf{g}_j^*$. Suppose that there does not exist such an l; then, $(\mathbf{g}_m^*)^T \mathbf{g}_j^{*\perp} = 0$ for all $m \in \mathcal{V}\backslash\{i, j\}$ and $(\mathbf{g}_i^*)^T \mathbf{g}_j^{*\perp} = -(\mathbf{g}_j^*)^T \mathbf{g}_i^{*\perp} > 0$. Thus, there does not exist any vector $\mathbf{g}_m^* \in \mathcal{B}_n$ such that $(\mathbf{g}_m^*)^T \mathbf{g}_j^{*\perp} < 0$, which contradicts the sufficiency assumption. This contradiction implies the existence of $l \in \mathcal{V}\backslash\{i, j, k\}$ such that $\mathbf{g}_l^* \neq \pm \mathbf{g}_j^*$ and $(\mathbf{g}_l^*)^T \mathbf{g}_j^{*\perp} < 0$. There are 3 possibilities as follows. (i) $(\mathbf{g}_l^*)^T \mathbf{g}_i^{*\perp} < 0$, we re-index $j \leftrightarrow l$, and move to Step 2. (ii) $(\mathbf{g}_l^*)^T \mathbf{g}_i^{*\perp} > 0$, we re-index $k \leftrightarrow l$, and move to Step 2. (iii) $(\mathbf{g}_l^*)^T \mathbf{g}_i^{*\perp} = 0$, ie, $\mathbf{g}_l^* = \pm \mathbf{g}_i^*$. Because $(\mathbf{g}_l^*)^T \mathbf{g}_j^{*\perp} < 0$ and $(\mathbf{g}_i^*)^T \mathbf{g}_j^{*\perp} > 0$, we have $\mathbf{g}_l^* = -\mathbf{g}_i^*$. Choosing $d_i = d_l = 1$, we write

$$\mathbf{g}_i^* + \mathbf{g}_l^* = \mathbf{0} \tag{6}$$

and move to Step 3.

Step 2: Since $\mathbf{g}_j^* \neq -\mathbf{g}_k^*$, 2 linearly independent vectors $\mathbf{g}_j^*$ and $\mathbf{g}_k^*$ form a basis for $\mathbb{R}^2$. Thus, we can write

$$\mathbf{g}_i^* = m_1 \mathbf{g}_j^* + m_2 \mathbf{g}_k^*, \tag{7}$$

where m_1 and m_2 are scalars. Premultiplying both sides of the above equation with $(\mathbf{g}_i^{*\perp})^T$ yields $0 = m_1 (\mathbf{g}_i^{*\perp})^T \mathbf{g}_j^* + m_2 (\mathbf{g}_i^{*\perp})^T \mathbf{g}_k^*$. Thus,

$$m_2 = m_1 \left(-\left(\mathbf{g}_i^{*\perp}\right)^T \mathbf{g}_j^*\right) / \left(\left(\mathbf{g}_i^{*\perp}\right)^T \mathbf{g}_k^*\right),$$

which implies that $sgn(m_1) = sgn(m_2)$. Thus, there are 2 cases as follows.

- Case 1: $m_1 < 0$, $m_2 < 0$. Thus, we can write $\mathbf{g}_i^* + r_1 \mathbf{g}_j^* + r_2 \mathbf{g}_k^* = \mathbf{0}$, where $r_1 = -m_1 > 0$ and $r_2 = -m_2 > 0$.
- Case 2: $m_1 > 0$, $m_2 > 0$. In this case, we will prove that there always exist at least 2 vectors $\mathbf{g}_{j_1}^*$, $\mathbf{g}_{k_1}^*, j_1, k_1 \in \mathcal{V}\backslash\{i\}$ such that $\mathbf{g}_i^* + r_1 \mathbf{g}_{j_1}^* + r_2 \mathbf{g}_{k_1}^* = \mathbf{0}$, where $r_1 > 0$, $r_2 > 0$.
  In fact, the 2 vectors $\mathbf{g}_i^*$ and $\mathbf{g}_i^{*\perp}$ separate the plane into 4 regions, ie, regions I to IV, as shown in Figure 3. If there does not exist even a single such pair j_1 and k_1, from Equation 7, all desired bearing vectors must be contained in 2 regions, ie, regions I and IV. Then, we can choose the index l corresponding to the vector $\mathbf{g}_l^*$ such that it minimizes the inner product $(\mathbf{g}_l^*)^T \mathbf{g}_i^{*\perp}$ (which is clearly negative from the assumption of the sufficiency proof). It follows that, for any vector $\mathbf{g}_k^* \in \mathcal{B}_n$, there are $c_1, c_2 \geq 0$ such that $\mathbf{g}_k^* = c_1 \mathbf{g}_l^* + c_2 \mathbf{g}_i^{*\perp}$ and

$$\left(\mathbf{g}_k^*\right)^T \mathbf{g}_l^{*\perp} = \left(c_1 \mathbf{g}_l^* + c_2 \mathbf{g}_i^{*\perp}\right)^T \mathbf{g}_l^{*\perp} = c_2 \left(\mathbf{g}_i^{*\perp}\right)^T \mathbf{g}_l^{*\perp} = c_2 \left(\mathbf{g}_i^*\right)^T \mathbf{J}^T \mathbf{J} \mathbf{g}_l^* = c_2 \left(\mathbf{g}_i^*\right)^T \mathbf{g}_l^* \geq 0.$$

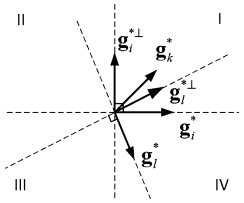

FIGURE 3 Four regions separated by 2 lines containing 2 vectors $\mathbf{g}_i^*$ and $\mathbf{g}_i^{*\perp}$

Thus, there does not exist any $\mathbf{g}_k^* \in \mathcal{B}_n$ such that $(\mathbf{g}_k^*)^T \mathbf{g}_l^{*\perp} < 0$. This contradicts our assumption, and thus, there must exist $j_1, k_1 \in \mathcal{V}\backslash\{i\}$ such that $\mathbf{g}_i^* + r_1\mathbf{g}_{j1}^* + r_2\mathbf{g}_{k1}^* = \mathbf{0}$, where $r_1, r_2 > 0$.

From both cases, it follows that, for any $\mathbf{g}_i^*$, we can always find 2 vectors $\mathbf{g}_j^*$ and $\mathbf{g}_k^*$ and scalars $r_1, r_2 > 0$ such that

$$\mathbf{g}_i^* + r_1\mathbf{g}_j^* + r_2\mathbf{g}_k^* = \mathbf{0}. \tag{8}$$

Step 3: Taking the summation over all i as expressed in the form of Equations 6 and 8, we obtain an expression in the form of Equation 3, which concludes the proof. □

In this paper, the control objective for the general $n-$agent scenario is to achieve a formation that satisfies a given set of desired bearings for the agents and not necessarily a fixed shape. As discussed earlier, only for $n = 3$, we get a fixed shape corresponding to a given set of desired bearing vectors, though the scale of the formation is not fixed in this case. Hence, we study the 3-agent scenario in some detail. Before stating the main problem, we now list some assumptions as follows.

Assumption 1. All agents' local reference frames are aligned, and the dynamics of each agent is given as in Equation 1.

Note that Assumption 1 is common in the bearing-based formation control problem. To relax this assumption, we could adopt some orientation alignment strategies simultaneously with the main control law (see for example the works of Zhao and Zelazo,[14] Oh and Ahn,[36] and Montijano et al[37]).

Assumption 2. Each agent $i (i \in \mathcal{V})$ is given a desired bearing vector, $\mathbf{g}_i^* \in \mathcal{B}_n$, with respect to its leader. Moreover, the set of desired bearing vector $\mathcal{B}_n$ is feasible.

We are now in a position to formally state the problem.

Problem 1. Given a group of n agents in a plane, satisfying Assumptions 1 and 2, and a feasible set of desired bearing vectors $\mathcal{B}_n$, design control laws for the agents using only bearing measurements such that $\mathbf{g}_i \to \mathbf{g}_i^*$ asymptotically, $\forall \mathbf{g}_i^* \in \mathcal{B}_n$.

2.2 | The bearing-only control law

To address the main problem, the bearing-only control law proposed in the work of Zhao and Zelazo[14] is adopted. Specifically, the control law for each agent i, $i = 1, \ldots, n$, is given by

$$\dot{\mathbf{p}}_i = \mathbf{u}_i = -\mathbf{P}_{\mathbf{g}_i}\mathbf{g}_i^*, \tag{9}$$

where $\mathrm{P}_{\mathbf{g}_i}$ is the projection matrix associated with the measured bearing vector $\mathbf{g}_i \in \mathbb{R}^d$ and is explicitly given by $\mathbf{P}_{\mathbf{g}_i} = \mathbf{I}_d - \mathbf{g}_i\mathbf{g}_i^T$. For each agent i, the control law (9) requires only a local bearing measurement $\mathbf{g}_i$ and a desired bearing vector $\mathbf{g}_i^*$.

Intuitively, if agent $i+1$ is stationary, the control law (9) asymptotically drives agent i to a position that satisfies $\mathbf{g}_i = \mathbf{g}_i^*$ while preserving the initial distance between 2 agents (see lemma 1 of the work of Trinh et al[20]).

Note that the projection matrix $\mathbf{P}_{\mathbf{g}_i}$ is symmetric, positive semidefinite, and idempotent, ie, $\mathbf{P}_{\mathbf{g}_i} = \mathbf{P}_{\mathbf{g}_i}^T = \mathbf{P}_{\mathbf{g}_i}^2$. Moreover, its null space is given by $\mathcal{N}(\mathbf{P}_{\mathbf{g}_i}) = \mathrm{Span}\{\mathbf{g}_i\}$ and the eigenvalues of $\mathrm{P}_{\mathbf{g}_i}$ are $\{0, 1, \ldots, 1\}$. In $\mathbb{R}^2$, the orthogonal projection matrix can be rewritten as $\mathbf{P}_{\mathbf{g}_i} = \mathbf{g}_i^{\perp}(\mathbf{g}_i^{\perp})^T$ [35] (see Lemma 6 and Corollary 1 for extension of this result to higher dimensions). As a result, we can also express the control law (9) as

$$\dot{\mathbf{p}}_i = -\mathbf{g}_i^{\perp}\left(\mathbf{g}_i^{\perp}\right)^T\mathbf{g}_i^*. \tag{10}$$

Remark 1. In this paper, we do not consider collision avoidance between neighboring agents. This assumption is necessary for all bearing-only–based formation control. In fact, the bearing vectors are undefined when 2 neighbor agents are collocated. Without distance measurements, each agent does not have enough information to avoid collisions. To tackle the lack of information in the bearing-only setup, several strategies have been proposed. These include treating collision avoidance separately using vision-based techniques[38] or restricting agents' initial positions to prevent collision.[14]

3 | THE DIRECTED CYCLE FORMATION IN THE PLANE

In this section, we study planar formations under the bearing-only control law (9). We focus on a special case in this class, ie, formations with 3 agents. The triangular formations in $\mathbb{R}^2$ possess a special property as discussed earlier. Their formation shapes are uniquely determined by specifying the desired bearing vectors. These shapes are only different up to a scaling factor. We obtain a sufficient condition on initial conditions for the 3-agent system such that the agents asymptotically achieve the desired bearing. Then, the general n-agent formations are discussed as a natural extension.

3.1 | The three-agent formations

The equations of motion for the 3-agent system can be explicitly written as follows:

$$\dot{\mathbf{p}}_1 = -\mathbf{P}_{\mathbf{g}_1}\mathbf{g}_1^* \tag{11a}$$

$$\dot{\mathbf{p}}_2 = -\mathbf{P}_{\mathbf{g}_2}\mathbf{g}_2^* \tag{11b}$$

$$\dot{\mathbf{p}}_3 = -\mathbf{P}_{\mathbf{g}_3}\mathbf{g}_3^*. \tag{11c}$$

We define the following sets:

$$\begin{aligned}\mathcal{Q}_3 &:= \left\{\mathbf{p} \in \mathbb{R}^6 | \mathbf{g}_i = \pm\mathbf{g}_i^*, i = 1,2,3\right\},\\ \mathcal{D}_3 &:= \left\{\mathbf{p} \in \mathbb{R}^6 | \mathbf{g}_i = \mathbf{g}_i^*, i = 1,2,3\right\},\\ \mathcal{U}_3 &:= \mathcal{Q}_3 \backslash \mathcal{D}_3.\end{aligned}$$

The set $\mathcal{Q}_3$ contains all equilibria of Equation 11 and can be partitioned into $\mathcal{D}_3$ that contains all desired formations and $\mathcal{U}_3$ containing the undesired ones. Figure 4 depicts an example of 2 different triangular formations in $\mathcal{Q}_3$. Since $\mathcal{B}_3$ is feasible, $\mathcal{D}_3 \neq \emptyset$, and there exists a triangle specified by 3 desired bearing vectors $\mathbf{g}_1^*$, $\mathbf{g}_2^*$, and $\mathbf{g}_3^*$. Thus, there exist positive scalars, ie, m_1, m_2, and m_3, such that

$$m_1\mathbf{g}_1^* + m_2\mathbf{g}_2^* + m_3\mathbf{g}_3^* = \mathbf{0}. \tag{12}$$

Dividing both sides of Equation 12 by $m_1 > 0$, we obtain

$$\mathbf{g}_1^* = -\frac{m_2}{m_1}\mathbf{g}_2^* - \frac{m_3}{m_1}\mathbf{g}_3^* = -n_2\mathbf{g}_2^* - n_3\mathbf{g}_3^*, \tag{13}$$

where $n_2 = m_2/m_1 > 0$ and $n_3 = m_3/m_1 > 0$. We examine the set of undesired equilibria $\mathcal{U}_3$ next.

Lemma 2. *The set $\mathcal{U}_3$ contains all points $\mathbf{p} \in \mathbb{R}^6$ such that $\mathbf{g}_i = -\mathbf{g}_i^*, i = 1,2,3$.*

Proof. Consider a point $\mathbf{p} \in \mathcal{U}_3$ where distances between 3 agents are $d_1, d_2, d_3 > 0$. Since $\sum_{i=1}^3 \mathbf{z}_i = \sum_{i=1}^3(\mathbf{p}_{i+1} - \mathbf{p}_i) = 0$ and $\mathbf{z}_i = d_i\mathbf{g}_i$, we have $d_1\mathbf{g}_1 + d_2\mathbf{g}_2 + d_3\mathbf{g}_3 = \mathbf{0}$, or equivalently, $\mathbf{g}_1 = -\frac{d_2}{d_1}\mathbf{g}_2 - \frac{d_3}{d_1}\mathbf{g}_3$. Without loss of generality, assume

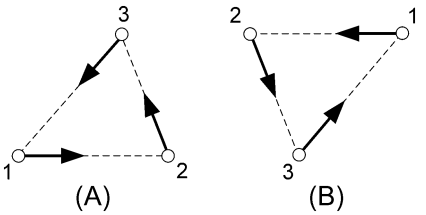

FIGURE 4 Formation A, is a desired formation, where $\mathbf{g}_i = \mathbf{g}_i^*$, $i = 1,2,3$, whereas formation B, is an undesired one, where $\mathbf{g}_i = -\mathbf{g}_i^*, i = 1,2,3$

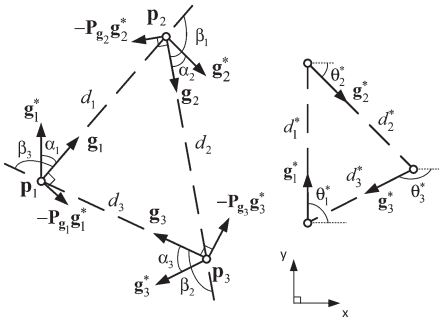

FIGURE 5 (Left) The directed triangle formation under the control law (11) and (right) a desired formation

that at $\mathbf{p}$, we have $\mathbf{g}_1 = -\mathbf{g}_1^*$. Then, we have

$$\mathbf{g}_1^* = \frac{d_2}{d_1}\mathbf{g}_2 + \frac{d_3}{d_1}\mathbf{g}_3. \tag{14}$$

Since $\mathbf{p} \in \mathcal{U}_3 \subset \mathcal{Q}_3$, it follows $\mathbf{g}_2 = \pm\mathbf{g}_2^*$, $\mathbf{g}_3 = \pm\mathbf{g}_3^*$. There are 4 possibilities as follows: (i) $\mathbf{g}_2 = -\mathbf{g}_2^*$, $\mathbf{g}_3 = -\mathbf{g}_3^*$; (ii) $\mathbf{g}_2 = \mathbf{g}_2^*$, $\mathbf{g}_3 = -\mathbf{g}_3^*$; (iii) $\mathbf{g}_2 = \mathbf{g}_2^*$, $\mathbf{g}_3 = -\mathbf{g}_3^*$; and (iv) $\mathbf{g}_2 = \mathbf{g}_2^*$, $\mathbf{g}_3 = \mathbf{g}_3^*$. Upon substituting these values of $\mathbf{g}_2$ and $\mathbf{g}_3$ for the 4 cases, in Equation 14, we get a unique representation of $\mathbf{g}_1^*$ in terms of $\mathbf{g}_2^*$ and $\mathbf{g}_3^*$ in each case because $\mathbf{g}_2^*$, $\mathbf{g}_3^*$, being linearly independent by definition, form a basis for $\mathbb{R}^2$. In other words, the representation of $\mathbf{g}_1^*$ in terms of $\mathbf{g}_2^*$ and $\mathbf{g}_3^*$ over the field of real numbers is unique. Furthermore, from Equation 13, we know that both of these scalars are negative. Hence, by comparing the representation (14) with Equation 13, it follows that only case (i) is possible for a feasible triangle. Therefore, we conclude that $\mathcal{U}_3 = \{\mathbf{p} \in \mathbb{R}^6 | \mathbf{g}_i = -\mathbf{g}_i^*, i = 1, 2, 3\}$. □

Consider a triangular formation in $\mathbb{R}^2$. Let α_i be the magnitude of the angle between $\mathbf{g}_i$ and $\mathbf{g}_i^*$, as depicted in Figure 5 ($0 \le \alpha_i \le \pi$). Then, at any equilibrium point of Equation 11 in $\mathcal{D}_3$, $\alpha_i = 0, \forall i = 1, 2, 3$, whereas at any equilibrium point in $\mathcal{U}_3$, $\alpha_i = \pi, \forall i = 1, 2, 3$. Thus, the convergence of $\mathbf{p}$ to a point in $\mathcal{D}_3$ (correspondingly $\mathcal{U}_3$) is equivalent to the convergence of $\alpha = [\alpha_1, \alpha_2, \alpha_3]^T$ to $[0, 0, 0]^T$ (correspondingly $[\pi, \pi, \pi]^T$). Let β_i ($0 \le \beta_i \le \pi$) be the magnitude of the angle between $\mathbf{g}_{i+1}$ and $\mathbf{g}_i$. In order to analyze the system's stability, we first change the position dynamics (11) into the angle dynamics. Since

$$\cos\alpha_i = \left(\mathbf{g}_i^*\right)^T \mathbf{g}_i, \tag{15}$$

taking the derivative with respect to time on both sides of Equation 15 and noting that

$$\frac{\partial \mathbf{g}_i}{\partial \mathbf{z}_i} = \frac{\partial}{\partial \mathbf{z}_i}\left(\frac{\mathbf{z}_i}{\|\mathbf{z}_i\|}\right) = \frac{\|\mathbf{z}_i\|\mathbf{I}_2 - \mathbf{z}_i\frac{\mathbf{z}_i^T}{\|\mathbf{z}_i\|}}{\|\mathbf{z}_i\|^2} = \frac{\mathbf{I}_2 - \mathbf{g}_i\mathbf{g}_i^T}{\|\mathbf{z}_i\|} = \frac{\mathbf{P}_{\mathbf{g}_i}}{d_i},$$

we get

$$\dot{\alpha}_i \sin\alpha_i = -\left(\mathbf{g}_i^*\right)^T \frac{\mathbf{P}_{\mathbf{g}_i}}{d_i}(\dot{\mathbf{p}}_{i+1} - \dot{\mathbf{p}}_i). \tag{16}$$

Substituting $\dot{\mathbf{p}}_i$ from Equation 10 and using the idempotent property of the projection matrix, $\mathbf{P}_{\mathbf{g}_i} = \mathbf{P}_{\mathbf{g}_i}^2 = \mathbf{g}_i^\perp(\mathbf{g}_i^\perp)^T$ in Equation 16, it follows that

$$\begin{aligned} d_i\dot{\alpha}_i \sin\alpha_i &= \left(\mathbf{g}_i^*\right)^T \mathbf{g}_i^\perp \left(\mathbf{g}_i^\perp\right)^T \mathbf{g}_{i+1}^\perp \left(\mathbf{g}_{i+1}^\perp\right)^T \mathbf{g}_{i+1}^* - \left(\mathbf{g}_i^*\right)^T \mathbf{g}_i^\perp \left(\mathbf{g}_i^\perp\right)^T \mathbf{g}_i^* \\ &= (\pm\sin\alpha_i)(\cos\beta_i)(\pm\sin\alpha_{i+1}) - \sin^2\alpha_i, \end{aligned}$$

where the last step is reached by using $(\mathbf{g}_i^*)^T\mathbf{g}_i^\perp = \pm\sin\alpha_i$ and $(\mathbf{g}_i^\perp)^T\mathbf{g}_{i+1}^\perp = \mathbf{g}_i^T\mathbf{J}^T\mathbf{J}\mathbf{g}_{i+1} = \mathbf{g}_i^T\mathbf{g}_{i+1} = \cos\beta_i$. Thus, the dynamics in terms of angles can be explicitly written as

$$\dot{\alpha}_1 = -\frac{\sin\alpha_1}{d_1} \pm \frac{\sin\alpha_2\cos\beta_1}{d_1}, \tag{17a}$$

$$\dot{\alpha}_2 = -\frac{\sin\alpha_2}{d_2} \pm \frac{\sin\alpha_3\cos\beta_2}{d_2}, \tag{17b}$$

$$\dot{\alpha}_3 = -\frac{\sin\alpha_3}{d_3} \pm \frac{\sin\alpha_1\cos\beta_3}{d_3}. \tag{17c}$$

Let θ_i^* be the absolute angle between the vector $\mathbf{g}_i^*$ and the x-axis of the global coordinate frame. It follows that the angle between $\mathbf{g}_i$ and the x-axis is $\theta_i^* \pm \alpha_i$. As a result, $\beta_i = (\theta_i^* \pm \alpha_i) - (\theta_{i+1}^* \pm \alpha_{i+1})$ is dependent on α_i and α_{i+1} only. Thus, we have the following relations:

$$\frac{\partial \dot{\alpha}_i}{\partial \alpha_i} = -\frac{\cos\alpha_i}{d_i} + \frac{\sin\alpha_i \pm \sin\alpha_{i+1}\cos\beta_i}{d_i^2}\frac{\partial d_i}{\partial \alpha_i} \pm \frac{\sin\alpha_{i+1}\sin\beta_i}{d_i}\frac{\partial \beta_i}{\partial \alpha_i}, \tag{18a}$$

$$\frac{\partial \dot{\alpha}_i}{\partial \alpha_{i+1}} = \left(\pm\frac{\cos\alpha_{i+1}\cos\beta_i}{d_i} + \frac{\sin\alpha_i \pm \sin\alpha_{i+1}\cos\beta_i}{d_i^2}\frac{\partial d_i}{\partial \alpha_{i+1}} \pm \frac{\sin\alpha_{i+1}\sin\beta_i}{d_i}\frac{\partial \beta_i}{\partial \alpha_{i+1}} \right), \tag{18b}$$

$$\frac{\partial \dot{\alpha}_i}{\partial \alpha_j} = \frac{\sin\alpha_i \pm \sin\alpha_{i+1}\cos\beta_i}{d_i^2}\frac{\partial d_i}{\partial \alpha_j},\ j \neq i, i+1. \tag{18c}$$

These aid in the linearization of the system (17) about the equilibria and subsequent local stability analysis. Toward the same end, we shall now state a refinement of Gershgorin's theorem in accordance with the work of Horn and Johnson.[39]

Lemma 3. *Suppose $G(\boldsymbol{A})$ is the union of the n Gershgorin disks for a matrix $\mathbf{A} \in \mathbb{R}^{n\times n}$. If the union of k of the n disks that comprise $G(\boldsymbol{A})$ forms a set $G_k(\boldsymbol{A})$ that is disjoint from the remaining $n-k$ disks, then $G_k(\boldsymbol{A})$ contains exactly k eigenvalues of $\boldsymbol{A}$, counted according to their algebraic multiplicities.*

Next, we investigate the local stability of the system described by Equation 17.

Lemma 4. *The equilibria corresponding to $\mathcal{D}_3$ are locally asymptotically stable, and the ones corresponding to $\mathcal{U}_3$ are unstable.*

Proof. At each equilibrium in $\mathcal{D}_3$, $\alpha_i = 0$, whereas at each equilibrium in $\mathcal{U}_3$, $\alpha_i = \pi$, $\forall i = 1,2,3$. By linearizing Equation 17, near the equilibrium $\alpha = [\alpha_1, \alpha_2, \alpha_3]^T = \mathbf{0}$,

$$\mathbf{A}_1 = \frac{\partial \dot{\alpha}}{\partial \alpha}\Big|_{\alpha=\mathbf{0}} = \begin{bmatrix} -\frac{1}{d_1^*} & \pm\frac{\cos\beta_1^*}{d_1^*} & 0 \\ 0 & -\frac{1}{d_2^*} & \pm\frac{\cos\beta_2^*}{d_2^*} \\ \pm\frac{\cos\beta_3^*}{d_3^*} & 0 & -\frac{1}{d_3^*} \end{bmatrix}.$$

Since the desired formation is not a straight line, $\beta_i^* \neq 0, \pi$ and the matrix $\mathbf{A}_1$ is strictly diagonally dominant. Thus, by Gershgorin's theorem (see theorem 6.1.10 of the work of Horn and Johnson[39]), $\mathbf{A}_1$ is Hurwitz. It follows that the equilibria in $\mathcal{D}_3$ are locally exponentially stable.

Similarly, near the equilibrium $\alpha = [\alpha_1, \alpha_2, \alpha_3]^T = [\pi, \pi, \pi]^T = \pi\mathbf{1}$, we have

$$\mathbf{A}_2 = \frac{\partial \dot{\alpha}}{\partial \alpha}\Big|_{\alpha=\pi\mathbf{1}} = \begin{bmatrix} \frac{1}{d_1^*} & \pm\frac{\cos\beta_1^*}{d_1^*} & 0 \\ 0 & \frac{1}{d_2^*} & \pm\frac{\cos\beta_2^*}{d_2^*} \\ \pm\frac{\cos\beta_3^*}{d_3^*} & 0 & \frac{1}{d_3^*} \end{bmatrix}.$$

In this case, $\mathbf{A}_2$ is again strictly diagonally dominant, so all its eigenvalues are in the right half of the complex plane. It follows that all equilibria in $\mathcal{U}_3$ are unstable. □

Theorem 1. *In $\mathbb{R}^2$, suppose that $0 \leq \alpha_i(0) \leq \frac{\pi}{2}$ for $i = 1,2,3$. Under Assumptions 1 and 2 and the control law (9), $\alpha \to \mathbf{0}$ asymptotically, ie, the agents asymptotically converge to a formation satisfying all the desired bearing vectors.*

Proof. Let $V = \|\alpha\|_\infty = \alpha_{\max} = \max_{i=1,2,3}\alpha_i$, which is continuous and positive definite. Since V is not continuously differentiable, we use Clark's generalized gradient and LaSalle's invariance principle for nonsmooth systems[40] to analyze the system given by Equation 17.

First, without loss of generality, assume that for an interval $t \in [T_1, T_2]$, $\alpha_1 > \alpha_2 \geq \alpha_3 \geq 0$. Then, $V = \max_{i=1,2,3}\alpha_i = \alpha_1$, and in this interval, from Equation 17, we have

$$\begin{aligned} \dot{V} = \dot{\alpha}_1 &= -\frac{1}{d_1}(\sin\alpha_1 \pm \sin\alpha_2\cos\beta_1) \\ &\leq -\frac{1}{d_1}(\sin\alpha_1 - \sin\alpha_2|\cos\beta_1|) \\ &< -\frac{1}{d_1}\sin\alpha_2(1 - |\cos\beta_1|) \leq 0. \end{aligned} \tag{19}$$

The last inequality holds, as $\sin(\cdot)$ is strictly increasing in its argument in $[0, \pi/2]$. Second, we consider the following case:

$$\max_i \alpha_i = \begin{cases} \alpha_1 & t \in [T_1, T_2), \\ \alpha_1 = \alpha_2 > \alpha_3 & t = T_2, \\ \alpha_2 & t \in (T_2, T_3]. \end{cases}$$

Based on the notation of Clark's generalized gradient,[40] we have $\partial V(\alpha) = [1, 0, 0]^T$ for $t \in [T_1, T_2)$, $\partial V(\alpha) = [0, 1, 0]^T$ for $t \in (T_2, T_3]$, and, at $t = T_2$,

$$\partial V(\alpha) = \overline{co}\left\{[1, 0, 0]^T, [0, 1, 0]^T\right\} = \left\{[\eta_1, \eta_2, 0]^T | \eta_i \in [0, 1], \eta_1 + \eta_2 = 1\right\},$$

where $\overline{co}\{a, b\}$ denotes the convex closure of a and b. Thus, $\dot{V}$ exists almost everywhere, and at $t = T_2$, we have $\dot{V} \in \dot{\tilde{V}}$, where

$$\begin{aligned} \dot{\tilde{V}} &= \bigcap_{\eta \in \partial V} \eta^T \begin{bmatrix} \dot{\alpha}_1 \\ \dot{\alpha}_2 \\ \dot{\alpha}_3 \end{bmatrix} = \eta_1 \dot{\alpha}_1 + \eta_2 \dot{\alpha}_2 + 0.\dot{\alpha}_3 \\ &= -\frac{\eta_1}{d_1}(\sin\alpha_1 \pm \sin\alpha_2 \cos\beta_1) - \frac{\eta_2}{d_2}(\sin\alpha_2 \pm \sin\alpha_3 \cos\beta_2) \\ &< -\frac{\eta_1}{d_1}\sin\alpha_2 (1 - |\cos\beta_1|) - \frac{\eta_2}{d_2}\sin\alpha_3 (1 - |\cos\beta_2|) \\ &\leq 0 \end{aligned}$$

for all $\eta_1 \in [0, 1]$, $\eta_2 \in [0, 1]$, and $\eta_1 + \eta_2 = 1$.

Similarly, consider the case as follows:

$$\max_i \alpha_i = \begin{cases} \alpha_1 & t \in [T_1, T_2), \\ \alpha_1 = \alpha_3 > \alpha_2 & t = T_2, \\ \alpha_3 & t \in (T_2, T_3]. \end{cases}$$

We have $\partial V(\alpha) = [1, 0, 0]^T$ for $t \in [T_1, T_2)$, $\partial V(\alpha) = [0, 0, 1]^T$ for $t \in (T_2, T_3]$, and, at $t = T_2$,

$$\partial V(\alpha) = \overline{co}\left\{[1, 0, 0]^T, [0, 0, 1]^T\right\} = \left\{[\eta_1, 0, \eta_3]^T | \eta_i \in [0, 1], \eta_1 + \eta_3 = 1\right\}.$$

Thus, $\dot{V}$ exists almost everywhere, and at $t = T_2$, $\dot{V} \in \dot{\tilde{V}}$, where

$$\begin{aligned} \dot{\tilde{V}} &= \bigcap_{\eta \in \partial V} \boldsymbol{\eta}^T \begin{bmatrix} \dot{\alpha}_1 \\ \dot{\alpha}_2 \\ \dot{\alpha}_3 \end{bmatrix} = \eta_1 \dot{\alpha}_1 + 0.\dot{\alpha}_2 + \eta_3 \dot{\alpha}_3 \\ &= -\frac{\eta_1}{d_1}(\sin\alpha_1 \pm \sin\alpha_2 \cos\beta_1) - \frac{\eta_3}{d_3}(\sin\alpha_3 \pm \sin\alpha_1 \cos\beta_3) \\ &= -\frac{\eta_1}{d_1}(\sin\alpha_1 \pm \sin\alpha_2 \cos\beta_1) - \frac{\eta_3}{d_3}(\sin\alpha_1 \pm \sin\alpha_1 \cos\beta_3) \\ &< -\frac{\eta_1}{d_1}\sin\alpha_2 (1 - |\cos\beta_1|) - \frac{\eta_3}{d_3}\sin\alpha_1 (1 - |\cos\beta_3|) \\ &\leq 0. \end{aligned}$$

Third, suppose that, at $t = T_4$, $\alpha_1 = \alpha_2 = \alpha_3$. Then, Clark's generalized gradient of V at $t = T_4$ is given by

$$\partial V(\alpha) = \overline{co}\left\{[1, 0, 0]^T, [0, 1, 0]^T, [0, 0, 1]^T\right\} = \left\{[\eta_1, \eta_2, \eta_3]^T | \eta_i \in [0, 1], \eta_1 + \eta_2 + \eta_3 = 1\right\}.$$

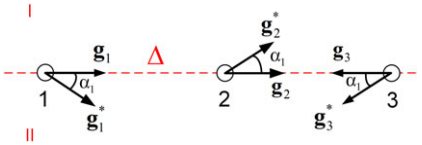

FIGURE 6 Illustration of the situation when 3 agents are collinear and $\alpha_1 = \alpha_2 = \alpha_3 > 0$ [Colour figure can be viewed at wileyonlinelibrary.com]

Then, $\dot{V} \in \dot{\tilde{V}}$, and since $\dot{\alpha}_i$ is continuous at $t = T_4$,

$$\begin{aligned}\dot{\tilde{V}} &= \bigcap_{\boldsymbol{\eta}\in\partial V} \boldsymbol{\eta}^T \begin{bmatrix}\dot{\alpha}_1\\ \dot{\alpha}_2\\ \dot{\alpha}_3\end{bmatrix} = \eta_1\dot{\alpha}_1 + \eta_2\dot{\alpha}_2 + \eta_3\dot{\alpha}_3\\ &= -\frac{\eta_1}{d_1}(\sin\alpha_1 \pm \sin\alpha_2\cos\beta_1) - \frac{\eta_2}{d_2}(\sin\alpha_2 \pm \sin\alpha_3\cos\beta_2)\\ &\quad -\frac{\eta_3}{d_3}(\sin\alpha_3 \pm \sin\alpha_1\cos\beta_3)\\ &\le -\sin\alpha_1 \sum_{i=1}^{3}\frac{\eta_i}{d_i}(1 - |\cos\beta_i|) \le 0 \end{aligned} \tag{20}$$

for all $\eta_i \in [0,1], \eta_1 + \eta_2 + \eta_3 = 1$.

From the above cases, we can conclude that V is a nonincreasing function of time and $0 \le \alpha_i \le \alpha_{\max} \le \alpha_{\max}(0) \le \pi/2$, $\forall t \ge 0$. Furthermore, $\dot{V} = 0$ can occur if and only if $\alpha_1 = \alpha_2 = \alpha_3$ and one of the following conditions holds.

- $\alpha_1 = \alpha_2 = \alpha_3 = 0$.
- There exists i such that $\beta_i = k\pi, k \in \{0,1\}$ and $\alpha_i \ne 0$. Without loss of generality, let $i = 1$. Then, agents 1, 2, and 3 are collinear in that order along a line Δ, as illustrated in Figure 6. In this case, we have $\beta_1 = 0$ and $\beta_2 = \beta_3 = \pi$. The line Δ separates the plane into 2 regions, ie, regions I and II. Suppose $\mathbf{g}_3^*$ points toward region II. Since $\alpha_1 = \alpha_3$ and $\mathbf{g}_1^* \ne \pm\mathbf{g}_3^*$, it follows that $\mathbf{g}_1^*$ must also point toward region II. Now, consider agent 2, if $\mathbf{g}_2^*$ points toward region I, since $\alpha_2 = \alpha_3$, it follows $\mathbf{g}_2^* = -\mathbf{g}_3^*$, which is a contradiction. On the other hand, if $\mathbf{g}_2^*$ points toward region II, since $\alpha_3 = \alpha_1$, it follows that $\mathbf{g}_2^* = \mathbf{g}_1^*$, which is also a contradiction. Thus, it is ruled out.

Consequently, $\dot{\tilde{V}} < 0$ whenever there exists i such that $\alpha_i > 0$ and $\dot{\tilde{V}} = 0$ if and only if $\alpha_i = 0, \forall i = 1,2,3$. It follows that $\alpha_i \to 0$ asymptotically.[40] □

3.2 | The *n*-agent formations

Similar to the 3-agent case, define the following sets:

$$\begin{aligned}\mathcal{Q}_n &:= \left\{\mathbf{p} \in \mathbb{R}^{2n} | \mathbf{g}_i = \pm\mathbf{g}_i^*, i = 1, \ldots, n\right\},\\ \mathcal{D}_n &:= \left\{\mathbf{p} \in \mathbb{R}^{2n} | \mathbf{g}_i = \mathbf{g}_i^*, i = 1, \ldots, n\right\},\\ \mathcal{U}_n &:= \mathcal{Q}_n \backslash \mathcal{D}_n.\end{aligned}$$

$\mathcal{Q}_n$ is the set of all equilibria of Equation 9 that can be partitioned into $\mathcal{D}_n$ (the set of desired equilibria) and $\mathcal{U}_n$ (the set of undesired equilibria). Unlike the 3-agent case, the undesired equilibrium set $\mathcal{U}_n$ may admit different possibilities and not just the set $\{\mathbf{p} \in \mathbb{R}^{2n} | \mathbf{g}_i = -\mathbf{g}_i^*, i = 1, \ldots, n\}$. Thus, Lemma 2 cannot be generalized for n-agents. Figure 7 shows an example of a 4-agent formation to illustrate this.

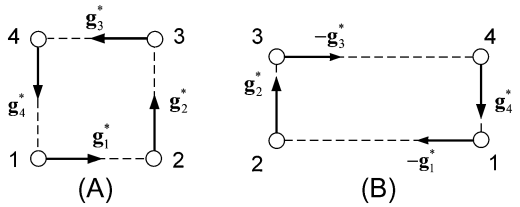

FIGURE 7 A desired formation is given in A. An undesired formation is given in B, where $\mathbf{g}_1 = -\mathbf{g}_1^*$, $\mathbf{g}_2 = \mathbf{g}_2^*$, $\mathbf{g}_3 = -\mathbf{g}_3^*$, and $\mathbf{g}_4 = \mathbf{g}_4^*$

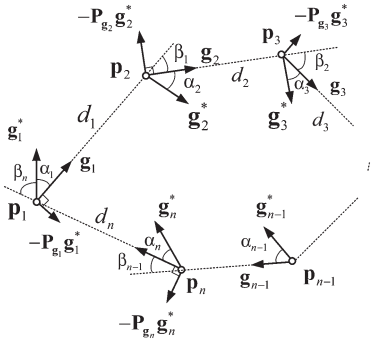

FIGURE 8 Formation of n agents under control law (9)

Consider a directed cycle formation in $\mathbb{R}^2$. As in the case of a triangle, let α_i be the magnitude of the angle between $\mathbf{g}_i$ and $\mathbf{g}_i^*$, as shown in Figure 8 and note that $0 \leq \alpha_i \leq \pi$. Each equilibrium $\mathbf{p}^* \in D$ corresponds to $\alpha_i = 0, i = 1, \ldots, n$. For each equilibrium $\mathbf{p}^* \in \mathcal{U}$, there exists at least an index i, $1 \leq i \leq n$ such that $\alpha_i = \pi$.

As in the 3-agent case, let β_i be the magnitude of the angle between $\mathbf{g}_i$ and $\mathbf{g}_{i+1}$ and $d_i = \|\mathbf{z}_i\|$ be the distance between agents i and $i+1$. The dynamics in terms of angles are given by

$$\dot{\alpha}_i = -\frac{\sin\alpha_i}{d_i} \pm \frac{\sin\alpha_{i+1}\cos\beta_i}{d_i}, \quad i = 1, \ldots, n. \tag{21}$$

Lemma 5. *The equilibria corresponding to $\mathcal{D}_n$ are locally asymptotically stable, whereas those corresponding to $\mathcal{U}_n$ are unstable.*

Proof. The proof is similar to that of Lemma 4. By linearizing Equation 21 near the corresponding equilibrium, we find that, at a desired equilibrium

$$\left.\frac{\partial\dot{\alpha}}{\partial\alpha}\right|_{\alpha=\mathbf{0}} = \begin{bmatrix} -\frac{1}{d_1^*} & \pm\frac{\cos\beta_1^*}{d_1^*} & 0 & \cdots & 0 \\ \vdots & \ddots & \ddots & \ddots & \vdots \\ \vdots & \vdots & \ddots & -\frac{1}{d_{m-1}^*} & \pm\frac{\cos\beta_{m-1}^*}{d_{m-1}^*} \\ \pm\frac{\cos\beta_m^*}{d_m} & 0 & \cdots & 0 & -\frac{1}{d_m^*} \end{bmatrix}$$

is Hurwitz according to Gershgorin's theorem, unless $\cos\beta_i^* = 1, \forall i$. However, this possibility is ruled out near an equilibrium since we know that, for a feasible formation, $\beta_i^* \neq 0$ for any i. On the other hand, for any equilibrium $\alpha = \alpha^*$ in $\mathcal{U}_n$, there exists at least some i, $1 \leq i \leq n$, such that $\alpha_i^* = \pi$. Thus, we have

$$\left.\frac{\partial\dot{\alpha}}{\partial\alpha}\right|_{\alpha=\alpha^*} = \begin{bmatrix} -\frac{1}{d_1^*} & \pm\frac{\cos\beta_1^*}{d_1^*} & 0 & \cdots & 0 \\ 0 & \ddots & \ddots & \ddots & 0 \\ \vdots & \ddots & \frac{1}{d_i^*} & \pm\frac{\cos\beta_i^*}{d_i^*} & 0 \\ 0 & \vdots & \ddots & \ddots & \ddots \\ \pm\frac{\cos\beta_m^*}{d_m^*} & 0 & \cdots & 0 & -\frac{1}{d_m^*} \end{bmatrix}$$

and observe that there always exists at least one Gershgorin disk in the open right half-plane (corresponding to the ith row). If there are more such rows with positive diagonal entries, then the disks corresponding to all such rows will be contained in the right half-plane. Moreover, all such disks in the right half-plane disk are disjoint from the disks in the left half-plane. Using the refinement stated in Lemma 3, it follows that there must be at least one eigenvalue with a positive real part if there is at least one positive diagonal entry in the Jacobian above. Thus, α^* is an unstable equilibrium. Hence, any undesired equilibrium in $\mathcal{U}_n$ is unstable. □

Theorem 2. *In $\mathbb{R}^2$, suppose that $0 \leq \alpha_i(0) \leq \frac{\pi}{2}$ for $i = 1, \ldots, n$. Under Assumptions 1 and 2 and the control law (9), $\alpha \to \mathbf{0}$ asymptotically, ie, the agents asymptotically converge to a formation satisfying all the desired bearing vectors.*

Proof. Consider the Lyapunov function $V = \|\alpha\|_{\max} = \max_{i=1,\ldots,n} \alpha_i$. By similar arguments as in Theorem 1, V is a decreasing function of time and $0 \leq \alpha_i \leq \alpha_{\max} \leq \alpha_{\max}(0) \leq \pi/2$, $\forall t \geq 0$. Furthermore, $\dot{V} = 0$ if and only if

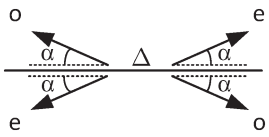

FIGURE 9 Four possible directions that the desired bearing vector makes an angle α with the line Δ

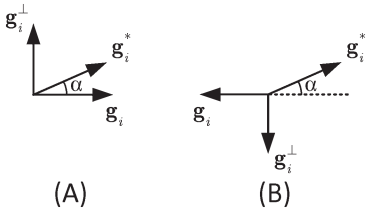

FIGURE 10 Vector $\mathbf{g}_i^*$ points northeast

$\alpha_i = \alpha_j \forall i,j = 1, \dots, n$ and one of the following conditions holds: (i) $\alpha_i = \alpha_j = 0, \forall i,j = 1, \dots, n$ or (ii) there exists a straight line in 2D such that all desired bearing vectors $\mathbf{g}_i^*$ are equally inclined with it by an angle α. In the following, we will prove that (ii) cannot happen and, thus, (i) is the only possible equilibrium.

Suppose that the agents have all aligned themselves in a straight line formation. Clearly, for a given α, there are only 4 possible directions, as illustrated in Figure 9. Without loss of generality, if one of the directions marked 'e' corresponds to an agent i such that i is even, then agent $(i+1)$ must have $\mathbf{g}_{i+1}^*$ along one of the directions marked 'o' because of the requirement that $\mathbf{g}_i^* \neq \pm\mathbf{g}_{i+1}^*$. Now, by mathematical induction, it follows that all agents with odd indices must be along one of the directions marked 'o' and all even indexed agents bearings must be along the directions marked 'e'. We split up the situation into 2 cases as follows.

Case 1. n is odd.
Consider the agent indexed n. Since n is odd, it must have its desired bearing $\mathbf{g}_n^*$ along one of the directions marked 'o'. However, agent $n+1$ (modulo n) or agent 1 also points along one of the directions marked 'o'. Thus, for odd n, we cannot have this scenario without violating Assumption 2.

Case 2. n is even.
Suppose n is even. Clearly, this does not pose the same problem as for the odd number of agents. Therefore, it is possible that agents do line up along a straight line Δ. However, we need to investigate if such a straight line formation is sustained. Consider the following equation:

$$d_i \sin\alpha_i \dot{\alpha}_i = \left(\mathbf{g}_i^*\right)^T \left(\mathbf{g}_i^\perp\right) \left(\mathbf{g}_i^\perp\right)^T \mathbf{g}_{i+1}^\perp \left(\mathbf{g}_{i+1}^\perp\right)^T \mathbf{g}_{i+1}^* - \left[\left(\mathbf{g}_i^*\right)^T \mathbf{g}_i^\perp\right]^2$$

when the agents are aligned along a straight line. Without loss of generality, we further suppose that the desired bearing of agent i is pointing toward northeast (NE), as shown in Figure 10. In Figure 10A, $(\mathbf{g}_i^*)^T\mathbf{g}_i^\perp = +\sin\alpha$, and in Figure 10B, $(\mathbf{g}_i^*)^T\mathbf{g}_i^\perp = -\sin\alpha$.

Now, consider the agent $(i+1)$. Figure 11 depicts 4 possible configurations of the bearings of agent $(i+1)$. Clearly, in Figure 11A,D, $(\mathbf{g}_{i+1}^*)^T\mathbf{g}_{i+1}^\perp = +\sin\alpha$, whereas in Figure 11B,C, $(\mathbf{g}_{i+1}^*)^T\mathbf{g}_{i+1}^\perp = -\sin\alpha$.

Now, for Figures 10A, 11A, and 11B taken together, $\cos\beta_i = (\mathbf{g}_i^\perp)^T\mathbf{g}_{i+1}^\perp = \mathbf{g}_i^T\mathbf{g}_{i+1} = \cos 0 = 1$, and for Figures 10A, 11C, and 11D taken together, $\cos\beta_i = \cos\pi = -1$. Similarly, for Figures 10B, 11A, and 11B, $\cos\beta_i = -1$, and for Figures 10B, 11C, and 11D taken together, $\cos\beta_i = 1$.

Keeping these in mind, it turns out that, for $\mathbf{g}_i^*$, as in Figure 10A,

$$\dot{\alpha}_i = \begin{cases} 0 & \text{for } \mathbf{g}_{i+1}^* \text{ as in Figures 11A and 11C} \\ -\frac{2\sin\alpha}{d_i} & \text{for } \mathbf{g}_{i+1}^* \text{ as in Figures 11B and 11D.} \end{cases}$$

Similarly, for $\mathbf{g}_i^*$, as in Figure 10B,

$$\dot{\alpha}_i = \begin{cases} 0 & \text{for } \mathbf{g}_{i+1}^* \text{ as in Figures 11A and 11C} \\ -\frac{2\sin\alpha}{d_i} & \text{for } \mathbf{g}_{i+1}^* \text{ as in Figures 11B and 11D.} \end{cases}$$

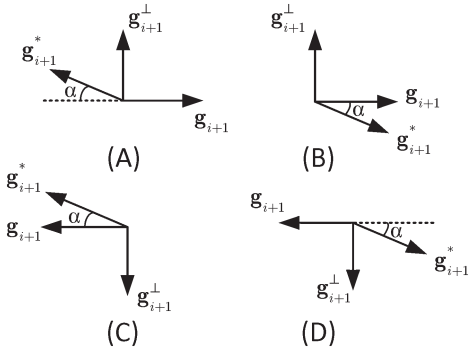

FIGURE 11 Four possible configurations of the bearings of agent (i+1)

Thus, if $\mathbf{g}_i^*$ points NE, $\mathbf{g}_{i+1}^*$ must point northwest (NW) for $\dot{\alpha}_i = 0$.

By a similar procedure, it may be shown that, if $\mathbf{g}_{i+1}^*$ points NW, then $\mathbf{g}_{i+2}^*$ must point NE for $\dot{\alpha}_{i+1} = 0$.

Combining these facts, it turns out that, if $\dot{\alpha}_i = 0, \forall i \in \mathcal{V}$ at the straight line formation is to hold true, then the sequence of desired bearings must be … - NE - NW - NE - NW - …. As a result, all desired bearing vectors are contained in a half-plane on the north side of the line Δ. This clearly violates Lemma 1 for the feasible desired bearing set. Hence, we conclude that, at the straight line configuration, there must be some i such that $\dot{\alpha}_i \neq 0$. Similar reasoning may be applied for $\mathbf{g}_i^*$ along any direction other than NE.

Hence, we conclude that, if the agents happen to align along a straight line for $t = t_1$, they cannot remain in this configuration $\forall t > t_1$. □

4 | THE TRIANGULAR FORMATION IN THE THREE-DIMENSIONAL SPACE

In this section, we extend the analysis on directed triangular formations to the 3-dimensional space. The directed triangular formations in the 3-dimensional space exhibit both similarities and uniqueness properties just as in the planar case. This extension also illustrates the challenges in analyzing system dynamics in a higher dimensional space and when the number of agents, n, is greater than 3.

4.1 | Preliminary results

Consider a group of 3 autonomous agents in $\mathbb{R}^3$. Each agent follows the bearing-only control law (9), where $\mathbf{P}_{\mathbf{g}_i} \in \mathbb{R}^{3\times3}$ is the projection matrix and $\mathbf{g}_i^* \in \mathbb{R}^3$ is the desired bearing vector of agent i. The following property holds for projection matrices.

Lemma 6. *Let $\mathbf{g}_i, \mathbf{g}_{i,1}, \mathbf{g}_{i,2} \in \mathbb{R}^3$ be a set of 3 orthonormal vectors. The following holds:*

$$\mathbf{P}_{\mathbf{g}_i} = \mathbf{I}_3 - \mathbf{g}_i\mathbf{g}_i^T = \mathbf{g}_{i,1}\mathbf{g}_{i,1}^T + \mathbf{g}_{i,2}\mathbf{g}_{i,2}^T. \tag{22}$$

Proof. Consider an arbitrary vector $\mathbf{u} \in \mathbb{R}^3$. From the definition of the 3 unit vectors $\mathbf{g}_i$, $\mathbf{g}_{i,1}$, and $\mathbf{g}_{i,2}$, these vectors form a basis in $\mathbb{R}^3$. Thus, we can write $\mathbf{u} = m_1\mathbf{g}_i + m_2\mathbf{g}_{i,1} + m_3\mathbf{g}_{i,2}$, where $m_l \in \mathbb{R}\ \forall l$. Observe that

$$\begin{aligned}\left(\mathbf{g}_i\mathbf{g}_i^T + \mathbf{g}_{i,1}\mathbf{g}_{i,1}^T + \mathbf{g}_{i,2}\mathbf{g}_{i,2}^T\right)\mathbf{u} &= \left(\mathbf{g}_i\mathbf{g}_i^T + \mathbf{g}_{i,1}\mathbf{g}_{i,1}^T + \mathbf{g}_{i,2}\mathbf{g}_{i,2}^T\right)(m_1\mathbf{g}_i + m_2\mathbf{g}_{i,1} + m_3\mathbf{g}_{i,2}) \\ &= m_1\mathbf{g}_i\mathbf{g}_i^T\mathbf{g}_i + m_2\mathbf{g}_{i,1}\mathbf{g}_{i,1}^T\mathbf{g}_{i,1} + m_3\mathbf{g}_{i,2}\mathbf{g}_{i,2}^T\mathbf{g}_{i,2} \\ &= m_1\mathbf{g}_i + m_2\mathbf{g}_{i,1} + m_3\mathbf{g}_{i,2} = \mathbf{u}.\end{aligned} \tag{23}$$

Since Equation 23 holds for any arbitrary $\mathbf{u} \in \mathbb{R}^3$, we have

$$\mathbf{g}_i\mathbf{g}_i^T + \mathbf{g}_{i,1}\mathbf{g}_{i,1}^T + \mathbf{g}_{i,2}\mathbf{g}_{i,2}^T = \mathbf{I}_3, \tag{24}$$

and Equation 22 follows immediately. □

In a similar manner, the result of Lemma 6 can be generalized to an arbitrary d-dimensional space ($d \geq 2$).

Corollary 1. *Let $\mathbf{g}_i$ and $\mathbf{g}_{i,1}, \ldots, \mathbf{g}_{i,d-1}$ be an orthonormal basis in $\mathbb{R}^d (d \geq 2)$. The following expression holds:*

$$\mathbf{P}_{\mathbf{g}_i} = \mathbf{I}_d - \mathbf{g}_i \mathbf{g}_i^T = \sum_{k=1}^{d-1} \mathbf{g}_{i,k} \mathbf{g}_{i,k}^T. \tag{25}$$

Since the set of desired bearing vectors $\mathcal{B}_3 = \{\mathbf{g}_i^* \in \mathbb{R}^3 | \|\mathbf{g}_i^*\| = 1, i = 1, 2, 3\}$ is *feasible*, there exist positive constants $d_1, d_2, and\ d_3$ such that

$$d_1 \mathbf{g}_1^* + d_2 \mathbf{g}_2^* + d_3 \mathbf{g}_3^* = \mathbf{0}. \tag{26}$$

Note that Equation 26 implies that the 3 desired bearing vectors $\mathbf{g}_1^*, \mathbf{g}_2^*$, and $\mathbf{g}_3^*$ are *coplanar*.

Next, we study the set of equilibria of Equation 9 for the 3-agent case. Define the following sets:

$$\begin{aligned} \bar{\mathcal{Q}}_3 &:= \left\{ \mathbf{p} \in \mathbb{R}^9 | \mathbf{g}_i = \pm \mathbf{g}_i^*, i = 1, 2, 3 \right\}, \\ \bar{\mathcal{D}}_3 &:= \left\{ \mathbf{p} \in \mathbb{R}^9 | \mathbf{g}_i = \mathbf{g}_i^*, i = 1, 2, 3 \right\}, \\ \bar{\mathcal{U}}_3 &:= \mathcal{Q}_3 \backslash \mathcal{D}_3, \end{aligned}$$

where the set $\bar{\mathcal{Q}}_3$ contains all equilibria of Equation 9, which includes $\bar{\mathcal{D}}_3$ (the set of all desired formations) and $\bar{\mathcal{U}}_3$ (the set of undesired formations). As before, $\bar{\mathcal{D}}_3 \neq \emptyset$, and there exists a triangle specified by the 3 desired bearing vectors $\mathbf{g}_1^*$, $\mathbf{g}_2^*$, and $\mathbf{g}_3^*$ since they comprise a feasible desired bearing set. We have the following lemma about the set of undesired equilibrium. The proof is similar to that of Lemma 2 by treating the plane on which the desired formation lies as $\mathbb{R}^2$.

Lemma 7. *The set $\bar{\mathcal{U}}_3$ contains all points $\mathbf{p} \in \mathbb{R}^9$ such that $\mathbf{g}_i = -\mathbf{g}_i^*, i = 1, 2, 3$.*

Remark 2. Note that the directed cycle graph with 4 agents, $\mathcal{C}_4$, in $\mathbb{R}^3$ can also be bearing rigid (see the work of Zhao et al[41] for a discussion) and is the counterpart of the triangle in $\mathbb{R}^2$. However, in the following subsection, we provide a result on local stability of general directed cycle formations in $\mathbb{R}^3$ and study asymptotic stability of the triangular formations in detail. The stability analysis of the 3-agent formation illustrates the challenges involved in analyzing the stability of more general formations in 3-dimensions.

4.2 | The dynamical model

Let α_i be the magnitude of the angle between $\mathbf{g}_i$ and $\mathbf{g}_i^*$ for $i = 1, 2, 3$. Since the 3 desired bearing vectors define a plane in $\mathbb{R}^3$, the shape of the triangle and the plane on which it lies are fixed whenever all 3 desired bearing vectors are satisfied. Thus, according to Lemma 7, the equilibria can be equivalently classified into 2 sets based on the angles α_i: $\bar{\mathcal{D}}_3 = \{\mathbf{p} \in \mathbb{R}^9 | \alpha_i = 0, i = 1, 2, 3\}$ and $\bar{\mathcal{U}}_3 = \{\mathbf{p} \in \mathbb{R}^9 | \alpha_i = \pi, i = 1, 2, 3\}$. Given a formation $\mathbf{p}(0) \in \mathbb{R}^9$, instead of the position dynamics (9), we can study the angle dynamics in terms of α_i. Toward this end, we transform Equation 9 into the angle dynamics. Figure 12 depicts the sensing model of agent i. It may be noted that, although the desired triangle is a planar polygon, the trajectories of the agents do not necessarily evolve along the plane on which the desired formation lies. In Figure 12, we denote the following.

- α_i: the magnitude of the angle between $\mathbf{g}_i$ and $\mathbf{g}_i^*$, $0 \leq \alpha_i \leq \pi$.
- $\mathcal{P}_i$: the plane having 2 tangent vectors $\mathbf{g}_{i,1}$ and $\mathbf{g}_{i,2}$, or in other words, the plane having $\mathbf{g}_i$ as its normal vector.
- $\nabla_i = \mathcal{P}_i \cap \mathcal{P}_{i+1}$: the intersection between planes $\mathcal{P}_i$ and $\mathcal{P}_{i+1}$.
- γ_i: the angle between the orthogonal projection of $\mathbf{g}_i^*$ into the plane $\mathcal{P}_i$ and $\mathbf{g}_{i,1}$, $0 \leq \gamma_i < 2\pi$.
- β_i: the magnitude of the angle between $\mathbf{g}_i$ and $\mathbf{g}_{i+1}$, $0 \leq \beta_i \leq \pi$.

For each $\alpha_i, i = 1, \ldots, n$, we can write

$$\cos \alpha_i = \left(\mathbf{g}_i^*\right)^T \mathbf{g}_i. \tag{27}$$

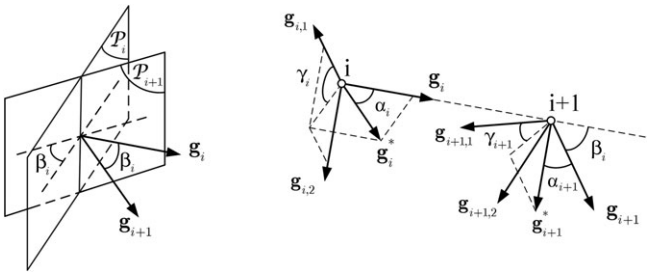

FIGURE 12 The sensing model of an agent i in the 3D space

Taking the derivative of both sides of Equation 27, it follows

$$\begin{aligned}\sin\alpha_i\dot{\alpha}_i &= -\mathbf{g}_i^{*T}\frac{\mathbf{P}_{\mathbf{g}_i}}{d_i}(\dot{\mathbf{p}}_{i+1}-\dot{\mathbf{p}}_i)\\ &= -\mathbf{g}_i^{*T}\frac{\mathbf{P}_{\mathbf{g}_i}}{d_i}\left(-\mathbf{P}_{\mathbf{g}_{i+1}}\mathbf{g}_{i+1}^*+\mathbf{P}_{\mathbf{g}_i}\mathbf{g}_i^*\right)\\ &= \mathbf{g}_i^{*T}\frac{\mathbf{P}_{\mathbf{g}_i}\mathbf{P}_{\mathbf{g}_{i+1}}}{d_i}\mathbf{g}_{i+1}^*-\mathbf{g}_i^{*T}\frac{\mathbf{P}_{\mathbf{g}_i}}{d_i}\mathbf{g}_i^*.\end{aligned}$$

Note that

$$\begin{aligned}\mathbf{g}_i^{*T}\mathbf{P}_{\mathbf{g}_i}\mathbf{g}_i^* &= \mathbf{g}_i^{*T}\left(\mathbf{g}_{i,1}\mathbf{g}_{i,1}^T+\mathbf{g}_{i,2}\mathbf{g}_{i,2}^T\right)\mathbf{g}_i^* = \left(\mathbf{g}_{i,1}^T\mathbf{g}_i^*\right)^2+\left(\mathbf{g}_{i,2}^T\mathbf{g}_i^*\right)^2\\ &= \sin^2\alpha_i\cos^2\gamma_i+\sin^2\alpha_i\sin^2\gamma_i = \sin^2\alpha_i(\cos^2\gamma_i+\sin^2\gamma_i) = \sin^2\alpha_i,\end{aligned}$$

and

$$\begin{aligned}\mathbf{g}_i^{*T}\mathbf{P}_{\mathbf{g}_i}\mathbf{P}_{\mathbf{g}_{i+1}}\mathbf{g}_{i+1}^* &= \mathbf{g}_i^{*T}\left(\mathbf{g}_{i,1}\mathbf{g}_{i,1}^T+\mathbf{g}_{i,2}\mathbf{g}_{i,2}^T\right)\left(\mathbf{g}_{i+1,1}\mathbf{g}_{i+1,1}^T+\mathbf{g}_{i+1,2}\mathbf{g}_{i+1,2}^T\right)\mathbf{g}_{i+1}^*\\ &= \left(\mathbf{g}_i^{*T}\mathbf{g}_{i,1}\mathbf{g}_{i,1}^T+\mathbf{g}_i^{*T}\mathbf{g}_{i,2}\mathbf{g}_{i,2}^T\right)\left(\mathbf{g}_{i+1,1}\mathbf{g}_{i+1,1}^T\mathbf{g}_{i+1}^*+\mathbf{g}_{i+1,2}\mathbf{g}_{i+1,2}^T\mathbf{g}_{i+1}^*\right)\\ &= \pm\left(\sin\alpha_i\cos\gamma_i\mathbf{g}_{i,1}^T+\sin\alpha_i\sin\gamma_i\mathbf{g}_{i,2}^T\right)\left(\mathbf{g}_{i+1,1}\sin\alpha_{i+1}\cos\gamma_{i+1}+\mathbf{g}_{i+1,2}\sin\alpha_{i+1}\sin\gamma_{i+1}\right)\\ &= \pm\sin\alpha_i\sin\alpha_{i+1}\left(\cos\gamma_i\mathbf{g}_{i,1}^T+\sin\gamma_i\mathbf{g}_{i,2}^T\right)(\mathbf{g}_{i+1,1}\cos\gamma_{i+1}+\mathbf{g}_{i+1,2}\sin\gamma_{i+1})\\ &= \pm\sin\alpha_i\sin\alpha_{i+1}h_i,\end{aligned} \tag{28}$$

where

$$h_i = \mathbf{w}_{i,1}^T\mathbf{w}_{i,2} = (\cos\gamma_i\mathbf{g}_{i,1}+\sin\gamma_i\mathbf{g}_{i,2})^T(\cos\gamma_{i+1}\mathbf{g}_{i+1,1}+\sin\gamma_{i+1}\mathbf{g}_{i+1,2}). \tag{29}$$

To ease the calculation of h_i, we choose $\mathbf{g}_{i+1,1}$ perpendicular to the line ∇_i and $\mathbf{g}_{i+1,2}$ lies along ∇_i as depicted in Figure 13. Let ψ_i be the angle between $\mathbf{g}_{i,1}$ and the orthogonal projection of $\mathbf{g}_{i+1,1}$ on the plane $\mathcal{P}_i$; then, $0 \le \psi_i < 2\pi$. We thus have $\mathbf{g}_{i,1}^T\mathbf{g}_{i+1,1} = |\cos\beta_i|\cos\psi_i$, $\mathbf{g}_{i,1}^T\mathbf{g}_{i+1,2} = \sin\psi_i$, $\mathbf{g}_{i,2}^T\mathbf{g}_{i+1,1} = |\cos\beta_i|\cos(\psi_i+\frac{\pi}{2}) = -|\cos\beta_i|\sin\psi_i$, and $\mathbf{g}_{i,2}^T\mathbf{g}_{i+1,2} = \cos\psi_i$. Substituting these into Equation 29, it follows

$$\begin{aligned}h_i &= |\cos\beta_i|\cos\gamma_i\cos\gamma_{i+1}\cos\psi_i+\cos\gamma_i\sin\gamma_{i+1}\sin\psi_i-|\cos\beta_i|\sin\gamma_i\cos\gamma_{i+1}\sin\psi_{i+1}+\sin\gamma_i\sin\gamma_{i+1}\cos\psi_i\\ &= |\cos\beta_i|\cos\gamma_{i+1}(\cos\gamma_i\cos\psi_i-\sin\gamma_i\sin\psi_i)+\sin\gamma_{i+1}(\cos\gamma_i\sin\psi_i+\sin\gamma_i\cos\psi_i)\\ &= |\cos\beta_i|\cos\gamma_{i+1}\cos(\gamma_i+\psi_i)+\sin\gamma_{i+1}\sin(\gamma_i+\psi_i).\end{aligned} \tag{30}$$

In Equation 30, applying the Cauchy-Schwarz inequality $(AX+BY)^2 \le (A^2+B^2)(X^2+Y^2)$, it follows

$$\begin{aligned}h_i^2 &\le (\cos^2\beta_i\cos^2\gamma_{i+1}+\sin^2\gamma_{i+1})\left(\cos^2(\gamma_i+\psi_i)+\sin^2(\gamma_i+\psi_i)\right)\\ &\le (1.\cos^2\gamma_{i+1}+\sin^2\gamma_{i+1}).1 = 1,\end{aligned} \tag{31}$$

with equality holding when $A/X = B/Y$. However, since $\sqrt{X^2+Y^2} = 1$, for $|h_i| = 1$, we also require $\sqrt{A^2+B^2} = 1$. Hence, from Equations 30 and 31, for $|h_i| = 1$, it is necessary that either (i) $|\cos\beta_i| = 1$ and $\gamma_{i+1} = \psi_i+\gamma_i$ or (ii) $|\cos\beta_i| \ne 1$

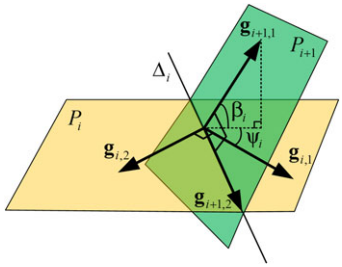

FIGURE 13 Illustration of vectors $\mathbf{g}_{i,1}$, $\mathbf{g}_{i,2}$, $\mathbf{g}_{i+1,1}$, and $\mathbf{g}_{i+1,2}$ [Colour figure can be viewed at wileyonlinelibrary.com]

and $\sin\gamma_{i+1} = \sin(\gamma_i + \psi_i) = 1$. Condition (i) implies $\beta_i = 0, \pi$, ie, $\mathbf{g}_i = \pm\mathbf{g}_{i+1}$. Condition (ii) implies $\gamma_{i+1} = \text{either}\frac{\pi}{2}$ or $\frac{3\pi}{2}$ for each i, and it follows further from Equation 30 that $\sin(\gamma_i + \psi_i) = 1$, ie, $\psi_i = 0$, or π.

Overall, we can write the dynamical equation of α_i for the 3-agent scenario as follows:

$$\dot{\alpha}_i = -\frac{\sin\alpha_i}{d_i} \pm h_i \frac{\sin\alpha_{i+1}}{d_i}, \tag{32}$$

where $|h_i| \leq 1$ for $i = 1, 2, 3$. It may be pointed out that, though Equation 32 involves more angle variables to describe the dynamics in 3 dimensions, it has a form similar to the 2-dimensional version (17) in Section 3.

4.3 | Stability analysis

We shall now study the system (32). As before, we note that

$$\frac{\partial\dot{\alpha}_i}{\partial\alpha_i} = -\frac{\cos\alpha_i}{d_i} + \frac{\sin\alpha_i \pm \sin\alpha_{i+1}h_i}{d_i^2}\frac{\partial d_i}{\partial\alpha_i} + \frac{\sin\alpha_{i+1}}{d_i}\frac{\partial h_i}{\partial\alpha_i}, \tag{33a}$$

$$\frac{\partial\dot{\alpha}_i}{\partial\alpha_{i+1}} = \pm\frac{\cos\alpha_{i+1}h_i}{d_i} + \frac{\sin\alpha_i \pm \sin\alpha_{i+1}h_i}{d_i^2}\frac{\partial d_i}{\partial\alpha_{i+1}} + \frac{\sin\alpha_{i+1}}{d_i}\frac{\partial h_i}{\partial\alpha_{i+1}}, \tag{33b}$$

$$\frac{\partial\dot{\alpha}_i}{\partial\alpha_j} = \frac{\sin\alpha_i \pm \sin\alpha_{i+1}h_i}{d_i^2}\frac{\partial d_i}{\partial\alpha_j} \pm \frac{\sin\alpha_{i+1}}{d_i}\frac{\partial h_i}{\partial\alpha_j},\ j \neq i, i+1. \tag{33c}$$

We are now equipped to prove the following result on local stability.

Lemma 8. *The equilibria corresponding to $\bar{\mathcal{D}}_3$ are locally asymptotically stable and the ones corresponding to $\bar{\mathcal{U}}_3$ are unstable.*

Proof. At each equilibrium in $\bar{\mathcal{D}}_3$, $\alpha_i = 0$, whereas at each equilibrium in $\bar{\mathcal{U}}_3$, $\alpha_i = \pi$, $\forall i = 1, 2, 3$. Denote $\alpha = [\alpha_1, \alpha_2, \alpha_3]^T$. Linearizing Equation 32, for 3 agents, at the equilibrium $\alpha = \mathbf{0}$

$$\mathbf{A}_1 = \left.\frac{\partial\dot{\alpha}}{\partial\alpha}\right|_{\alpha=\mathbf{0}} = \begin{bmatrix} -\frac{1}{d_1^*} & \pm\frac{h_1^*}{d_1^*} & 0 \\ 0 & -\frac{1}{d_2^*} & \pm\frac{h_2^*}{d_2^*} \\ \pm\frac{h_3^*}{d_3^*} & 0 & -\frac{1}{d_3^*} \end{bmatrix}.$$

In order to use Gershgorin's theorem, we have to ensure that $|h_i^*| < 1$ at the equilibrium point. However, the diagonally dominant Jacobian, $\mathbf{A}_1$, satisfies the 'SC-property' as mentioned in the work of Horn and Johnson.[39] Thus, according to theorem 6.2.8 and corollary 6.2.9 in the work of Horn and Johnson,[39] if the Jacobian $\mathbf{A}_1$ has to have an eigenvalue at the origin, then $|h_i| = 1\ \forall i$ is required. Therefore, it suffices to ensure that $|h_i| = 1$ cannot hold for at least some i. However, we can, in fact, show that $|h_i| < 1\ \forall i$. From the assumption that $\mathbf{g}_i^* \neq \mathbf{g}_{i+1}^*, \forall i$, it follows that $|\cos\beta_i^*| \neq 1$ or condition (i) cannot occur for all i, ie, $\beta_i^* = 0, \pi$ cannot hold for any i. Moreover, condition (ii) also cannot hold because, at the equilibrium, $\gamma_i = 0\ \forall i$. This is true since the projection of $\mathbf{g}_i = \mathbf{g}_i^*$ on the plane $\mathcal{P}_i$ is zero for all i. Thus, from Equation 29 and the discussion following it, at equilibrium, $\alpha = \mathbf{0}$, and we have $|h_i^*| = |\cos\beta_i^*\cos\psi_i^*| < 1\ \forall i$. In fact, for a triangle (a planar polygon), at equilibrium, we have $\psi_i^* = 0\ \forall i$, so the off-diagonal entries of $\mathbf{A}_1$ are the same as that obtained for the 2-dimensional case. Thus, the matrix $\mathbf{A}_1$ is strictly diagonally dominant with negative diagonal entries and is therefore Hurwitz by Gershgorin's theorem.[39] It follows that the equilibrium $\alpha = \mathbf{0}$ is locally exponentially stable.

Similarly, at the equilibrium $\alpha = [\alpha_1, \alpha_2, \alpha_3]^T = [\pi, \pi, \pi]^T = \pi\mathbf{1}$, we have

$$\mathbf{A}_2 = \frac{\partial \dot{\alpha}}{\partial \alpha}\Big|_{\alpha=\pi\mathbf{1}} = \begin{bmatrix} \frac{1}{d_1^*} & \pm\frac{h_1^*}{d_1^*} & 0 \\ 0 & \frac{1}{d_2^*} & \pm\frac{h_2^*}{d_2^*} \\ \pm\frac{h_3^*}{d_3^*} & 0 & \frac{1}{d_3^*} \end{bmatrix}.$$

In this case, $\mathbf{A}_2$ is again strictly diagonally dominant, so all its eigenvalues are in the right half of the complex plane. It follows that all equilibria in $\mathcal{U}_3$ are unstable. □

We shall now state another lemma that will aid in analyzing the region of attraction of the desired equilibria.

Lemma 9. *Suppose 3 coplanar unit vectors $\mathbf{v}_i \in \mathbb{R}^3, i = 1, 2, 3$, which are pairwise linearly independent, satisfy $\sum_{i=1}^3 \lambda_i \mathbf{v}_i = 0$ for $\lambda_i \in \mathbb{R}_+$. A fourth unit vector $\mathbf{v} \in \mathbb{R}^3$ that subtends equal angles with each $\mathbf{v}_i$ must be normal to the plane containing the 3 vectors.*

Proof. Consider $\mathbf{v}^T \sum_{i=1}^3 \lambda_i \mathbf{v}_i = 0$. Now, $|\mathbf{v}^T \mathbf{v}_i| = c \in \mathbb{R}_+ \, \forall i$. Thus, we have $c(\pm\lambda_1 \pm \lambda_2 \pm \lambda_3) = 0$. Since $\mathbf{v}_i$ is pairwise linearly independent and satisfy $\sum_{i=1}^3 \lambda_i \mathbf{v}_i = 0$, these vectors define triangles in their common plane, each of whose sides has lengths equal or proportional to λ_i with the constant of proportionality describing the size of the particular triangle. Furthermore, we know that, for a triangle, the sum of the length of 2 sides is always greater than the third. Therefore, $(\pm\lambda_1 \pm \lambda_2 \pm \lambda_3) \neq 0$. Thus, $c = 0$. Hence the result is proved. □

Theorem 3. *In $\mathbb{R}^3$, suppose that $0 \leq \alpha_i(0) \leq \frac{\pi}{2}$ for $i = 1, 2, 3$. Under the control law (9), $\alpha \to \mathbf{0}$ asymptotically, ie, the agents asymptotically converge to a formation satisfying all the desired bearing vectors.*

Proof. Consider the Lyapunov function $V = \|\alpha\|_\infty = \max_{i=1,2,3} \alpha_i$, by similar arguments as in Theorem 1, V is a decreasing function of time and $0 \leq \alpha_i \leq \alpha_{\max} \leq \alpha_{\max}(0) \leq \pi/2, \forall t \geq 0$. Furthermore, $\dot{V} = 0$ if and only if $\alpha_1 = \alpha_2 = \alpha_3$ and one of the following conditions holds.

1. $\alpha_1 = \alpha_2 = \alpha_3 = 0$.
2. There exists a configuration such that $|h_i| = 1, \forall i$. Then, the following possibilities emerge.
   (a) $\beta_i = 0$ or π, and $\gamma_{i+1} = \gamma_i + \psi_i$ for all i.
   (b) $\gamma_i =$ either $\frac{\pi}{2}$ or $\frac{3\pi}{2}$, and $\psi_i = 0, \pi$ for each i.
   (c) $\beta_i = 0$ or π and $\gamma_{i+1} = \gamma_i + \psi_i$ for some i, whereas $\gamma_j = \frac{\pi}{2}$ or $\frac{3\pi}{2}$ and $\psi_j = 0$ or π for the remaining $j \in \mathcal{V}, j \neq i$.

We will prove that each of the cases (a), (b), and (c) cannot hold.

1. In this case, 3 agents are collinear because of $\beta_i = 0$ or π for $i = 1, 2, 3$. Furthermore, the 3 desired bearing vectors are coplanar (because they are feasible) and $\alpha_1 = \alpha_2 = \alpha_3 = \alpha \neq 0$. Now, following Lemma 9, we may conclude that $\alpha = \pi/2$ and the agents are aligned along the normal to the plane containing the desired bearing vectors. Thus, the planes $\mathcal{P}_i$ are identical for all i. This is also the same plane on which all the desired bearing vectors lie. Now, consider the expression for h_i in Equation 29. From the definition of γ_i, it is clear that, in this case, the vectors $\mathbf{w}_{i,1}$ and $\mathbf{w}_{i,2}$ are the unit vectors $\mathbf{g}_i^*$ and $\mathbf{g}_{i+1}^*$, respectively, because the orthogonal projections of $\mathbf{g}_i^*$ and $\mathbf{g}_{i+1}^*$ on $\mathcal{P}_i$ (or $\mathcal{P}_{i+1}$) are the vectors $\mathbf{g}_i^*$ and $\mathbf{g}_{i+1}^*$ themselves. Since $\mathbf{g}_i^* \neq \pm\mathbf{g}_{i+1}^*$ for a feasible formation, we conclude that $|h_i|$, which is the inner product of 2 linearly independent unit vectors, must be less than unity for all i. Alternately, we could arrive at the same conclusion about $|h_i|$ by observing that the requirement $\gamma_{i+1} = \gamma_i + \psi_i$ also leads to $\mathbf{g}_i^* = \pm\mathbf{g}_{i+1}^*$ because, now, $\mathbf{g}_{i,1}$ and $\mathbf{g}_{i+1,1}$, being coplanar, are separated by the angle ψ_i. This is clearly infeasible, leading to a contradiction.
2. In this case, it is clear from Figure 13 that $\psi_i = 0, \pi \, \forall i$ leads to $\mathbf{g}_{i,2} = \pm\mathbf{g}_{i+1,2} \, \forall i$. Since we have chosen $\mathbf{g}_{i+1,2}$ to lie along ∇_i, ie, the line of intersection of $\mathcal{P}_i$ and $\mathcal{P}_{i+1}$, it immediately follows that all the planes $\mathcal{P}_i$ intersect along the same line, eg, ∇, as shown in Figure 14A. In addition, since $\gamma_i =$ either $\frac{\pi}{2}$ or $\frac{3\pi}{2}$ for each i, we conclude from the definition of γ_i that the 3 vectors $\mathbf{g}_i^*, \mathbf{g}_i$ and $\mathbf{g}_{i,2}$ are all orthogonal to $\mathbf{g}_{i,1}$ and hence coplanar for all i. It may be remarked that even if $\gamma_i = \frac{\pi}{2}$ while $\gamma_{i+1} = \frac{3\pi}{2}$, the coplanarity of $\mathbf{g}_i^*, \mathbf{g}_i$, and $\mathbf{g}_{i,2}$ still holds. In other words, all γ_i need not necessarily be equal as long as they are either $\frac{\pi}{2}$ or $\frac{3\pi}{2}$ individually; our conclusion about the coplanarity is unaffected.

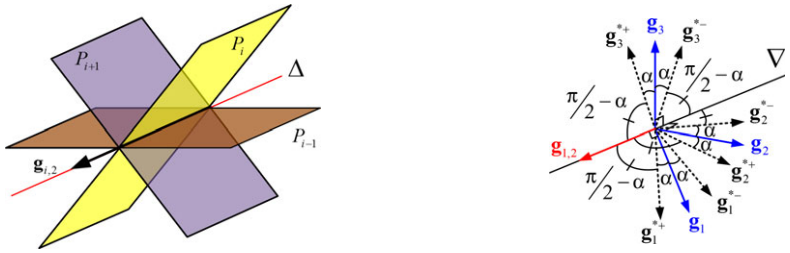

(A) All planes $\mathcal{P}_i$ intersect on the line ∇. (B) $\mathbf{g}_i, \mathbf{g}_{i-1}$, and $\mathbf{g}_{i+1}$ are perpendicular to ∇.

FIGURE 14 Illustration of the proof of Theorem 3 [Colour figure can be viewed at wileyonlinelibrary.com]

Denote the plane containing the triplets $\mathbf{g}_i^*, \mathbf{g}_i$, and $\mathbf{g}_{i,2}$ as $\mathcal{P}_i^\perp$. Note that all such planes $\mathcal{P}_i^\perp$ also intersect along the common line ∇, containing $\mathbf{g}_{i,2}$. Since $\alpha_i = \alpha \neq 0\,\forall i$, we may now deduce that, for each i, $\mathbf{g}_i^*$ has 2 possible orientations on the plane $\mathcal{P}_i^\perp$ for a given $\mathbf{g}_i$. This is illustrated in Figure 14B. For one of these orientations, $\mathbf{g}_{1,2}^T\mathbf{g}_i^* > 0$ whereas for the other, $\mathbf{g}_{1,2}^T\mathbf{g}_i^* < 0$. Since there exist scalars $d_i > 0$ such that $\sum_{i=1}^3 d_i\mathbf{g}_i^* = 0$, it follows $\mathbf{g}_{1,2}^T\mathbf{g}_i^*$ cannot all be positive or negative because, otherwise, $\mathbf{g}_{i,2}^T(\sum_{i=1}^3 d_i\mathbf{g}_i^*) \neq 0$ for any choice of the scalars d_i. Thus, the desired $\mathbf{g}_i^*$ bearings can neither all be pointing toward $\mathbf{g}_i^{*+}$ nor all be pointing toward $\mathbf{g}_i^{*-}$ in Figure 14B. In other words, we may conclude that, in Equation 28, the orthogonal projection of $\mathbf{g}_i^*$ on $\mathcal{P}_i$, ie, $\mathbf{P}_{\mathbf{g}_i}\mathbf{g}_i^*$ and that of $\mathbf{g}_{i+1}^*$ on $\mathcal{P}_{i+1}$, ie, $\mathbf{P}_{\mathbf{g}_{i+1}}\mathbf{g}_{i+1}^*$, both of which lie on the line ∇ that is common to all the planes $\mathcal{P}_i$, cannot point along the same direction for all i. Hence, the inner product of these 2 projections, $\mathbf{g}_i^{*T}\mathbf{P}_{\mathbf{g}_i}\mathbf{P}_{\mathbf{g}_{i+1}}\mathbf{g}_{i+1}^*$, must be negative for some i. Thus, for some i, the product $\pm\sin\alpha_i\sin\alpha_{i+1}$ must be $-\sin\alpha_i\sin\alpha_{i+1} = -\sin^2\alpha$. This is because there must be some i such that $\mathbf{g}_i^*$ points along $\mathbf{g}_i^{*+}$ while $\mathbf{g}_{i+1}^*$ is along $\mathbf{g}_{i+1}^{*-}$ or vice versa. At the same time, for 3 agents, there will also be some j such that the product $\pm\sin\alpha_j\sin\alpha_{j+1}$ must be $+\sin\alpha_j\sin\alpha_{j+1} = +\sin^2\alpha$. Hence, there exists i such that its dynamics will be

$$\dot{\alpha}_i = \frac{2\sin\alpha}{d_i} \neq 0.$$

In addition, j such that its dynamics will be

$$\dot{\alpha}_j = 0.$$

This nonzero derivative of α_i will cause it to change the value of α_i whereas the zero derivative of α_j will cause α_j to remain unchanged. This will violate the condition $\alpha_i = \alpha\,\forall i$, and thus, $\dot{V}$ will not remain zero.

3. In this case, since there are only 3 agents, $\beta_i = 0$ again implies that 3 agents are collinear. Thus, it reduces to the same scenario as in (a).

From above arguments, (ii) cannot happen, and thus, $\dot{V} = 0$ if and only if (i) happens or 3 agents are at the desired formation. It follows from the LaSalle invariance principle that the desired equilibrium is asymptotically stable. □

4.4 | The *n*-agent case

We now briefly consider the case of an n-agent system in $\mathbb{R}^3$. As before, we define the following sets:

$$\bar{\mathcal{Q}}_n = \left\{\mathbf{p} \in \mathbb{R}^{3n} | \mathbf{g}_i = \pm\mathbf{g}_i^*\right\},$$
$$\bar{\mathcal{D}}_n = \left\{\mathbf{p} \in \mathbb{R}^{3n} | \mathbf{g}_i = \mathbf{g}_i^*\right\},$$
$$\bar{\mathcal{U}}_n = \bar{\mathcal{Q}}_n \backslash \bar{\mathcal{D}}_n.$$

The following lemma is about the local stability of equilibrium sets $\bar{\mathcal{D}}_n$ and $\bar{\mathcal{U}}_n$.

Lemma 10. *The equilibria corresponding to $\bar{\mathcal{D}}_n$ are locally asymptotically stable, and the ones corresponding to $\bar{\mathcal{U}}_n$ are unstable.*

Proof. Linearizing Equation 32, for n agents, at the equilibrium $\alpha = \mathbf{0}$,

$$\mathbf{A}_1 = \left.\frac{\partial \dot{\alpha}}{\partial \alpha}\right|_{\alpha=\mathbf{0}} = \begin{bmatrix} -\frac{1}{d_1^*} & \pm\frac{h_1^*}{d_1^*} & 0 & \cdots & 0 \\ 0 & -\frac{1}{d_2^*} & \pm\frac{h_2^*}{d_2^*} & \cdots & 0 \\ \vdots & \vdots & \ddots & \vdots & \vdots \\ 0 & 0 & 0 & \cdots & \pm\frac{h_{n-1}^*}{d_{n-1}^*} \\ \pm\frac{h_n^*}{d_n^*} & 0 & 0 & \cdots & -\frac{1}{d_n^*} \end{bmatrix}.$$

Following a same argument as in Lemma 8, we can prove that the Jacobian $\mathbf{A}_1$ is strictly diagonally dominant at the equilibria corresponding to $\bar{\mathcal{D}}_n$ and is thus Hurwitz. Similarly, the Jacobian at the equilibria corresponding to $\bar{\mathcal{U}}_n$ has all its eigenvalues in the right half-plane, and thus, they correspond to unstable equilibria. □

Remark 3. It may be noted that it is not straightforward to prove the asymptotic stability of the equilibrium in $\bar{\mathcal{D}}_n$. Consider the Lyapunov function $V = \max_{i=1,\dots,n}\alpha_i$, we can process in a similar manner as in Theorem 3 until the step of examining all possibilities that may lead to $\dot{V} = 0$. At that point, we cannot deduce collinearity of the n-agent formation as in case (c) in the proof of Theorem 3.

5 | SIMULATIONS

5.1 | Simulation 1: A three-agent formation in $\mathbb{R}^2$

In this simulation, we consider 3 agents. The desired formation is an equilateral triangle. The initial positions of the agents are $\mathbf{p}_1(0) = [0, 0]^T$, $\mathbf{p}_2(0) = [1.5, -1]^T$, and $\mathbf{p}_3(0) = [2, 1.5]^T$, as shown in Figure 15A. It may be verified that the condition for convergence is satisfied.

The trajectories of the 3 agents are shown in Figure 15B. The agents asymptotically form an equilateral triangle as desired. Observe from Figure 15C that the angle α_i converges to 0 asymptotically as $t \to \infty$.

For the same system with another initial condition that does not satisfy our condition $\alpha_i \leq \frac{\pi}{2}\ \forall i$, it is shown in Figure 16 that instability can occur. Thus, the simulation results are consistent with our analysis in Section 3.1.

5.2 | Simulation 2: A six-agent formation in $\mathbb{R}^2$

Next, we consider a 6-agent system with the measurement graph, as depicted in Figure 1. The desired bearing vectors are chosen to obtain a regular hexagon. The initial positions of the agents are chosen such that they are not too far from the desired bearings.

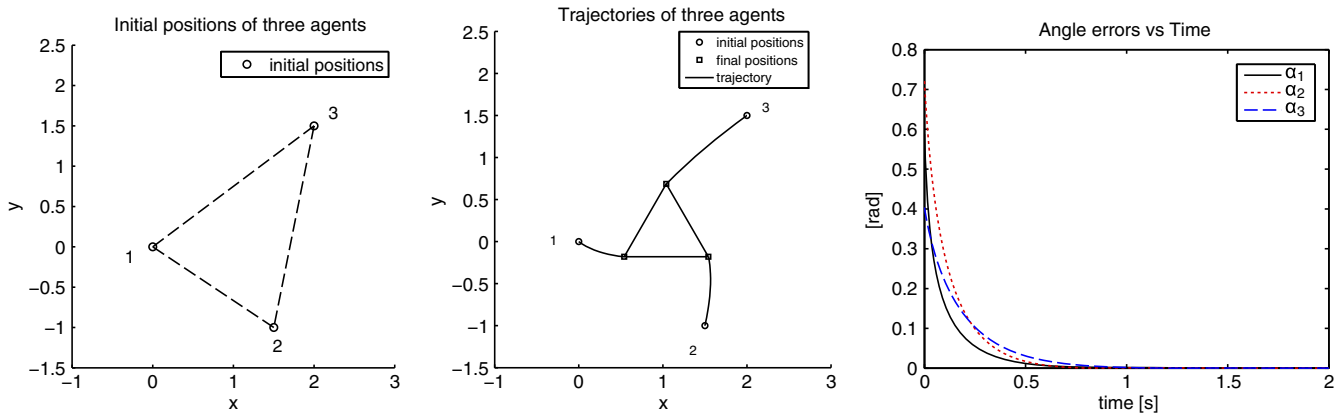

(A) The initial formation. (B) Trajectories and final formation. (C) The angles α_i vs. Time [s].

FIGURE 15 Simulation results of a 3-agent formation under the bearing-only control law (9) [Colour figure can be viewed at wileyonlinelibrary.com]

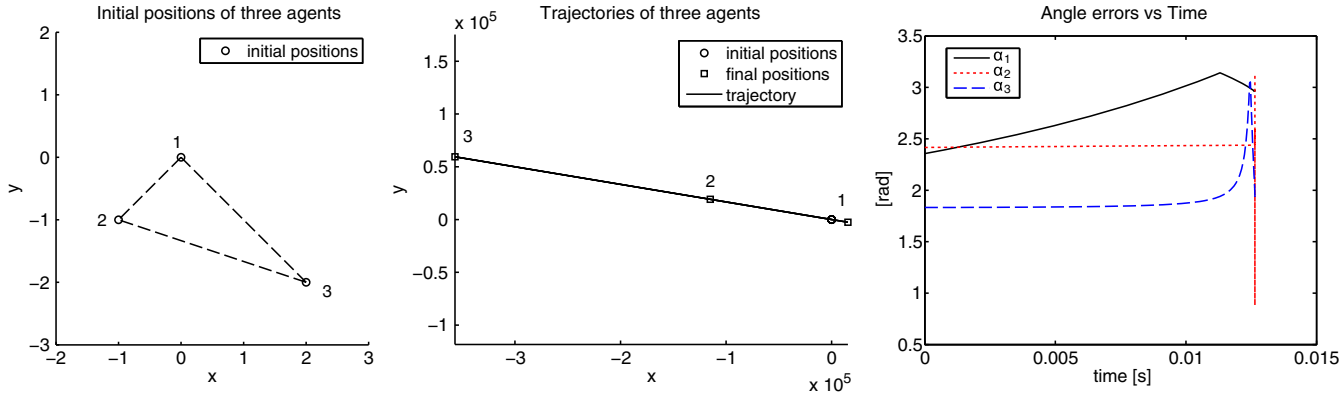

(A) The initial formation. (B) Trajectories of three agents. (C) The angles α_i vs. time [s].

FIGURE 16 The 3-agent formation under the bearing-only control law (9) with another initial condition [Colour figure can be viewed at wileyonlinelibrary.com]

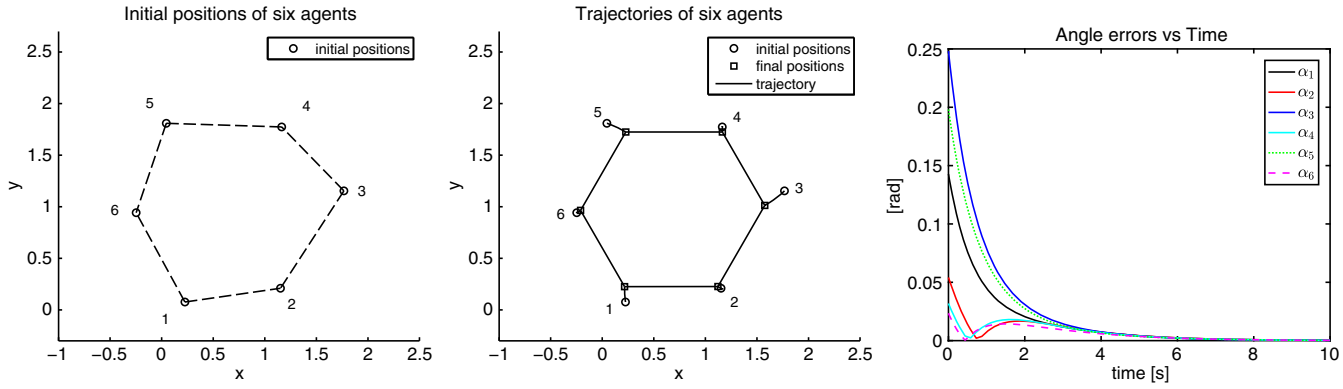

(A) The initial formation. (B) Trajectories and final formation. (C) The angles α_i vs. time.

FIGURE 17 Simulation results of a 6-agent formation under the bearing-only control law (9) [Colour figure can be viewed at wileyonlinelibrary.com]

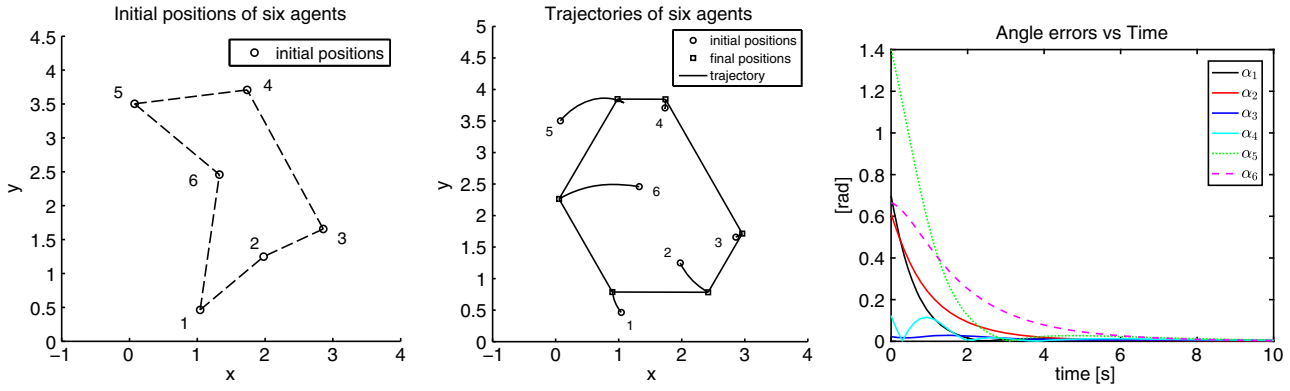

(A) The initial formation. (B) Trajectories and final formation. (C) The angles α_i vs. time.

FIGURE 18 Simulation results of the 6-agent formation for a different set of initial conditions [Colour figure can be viewed at wileyonlinelibrary.com]

Two simulations with different initial conditions, both satisfying $\alpha_i \leq \frac{\pi}{2}\ \forall i$, are shown in Figures 17 and 18. In both simulations, the agents asymptotically converge to a formation that satisfies the desired bearing vector set $\mathcal{B}_n$. The maximum angle $\alpha_{\max}$ asymptotically decays, as can be seen from Figures 17C and 18C. Observe from Figures 17B and 18B that the final formation shape is not fixed. This further shows that for $n > 3$, the shape of the C_n-formation is not uniquely determined by specifying bearings alone.

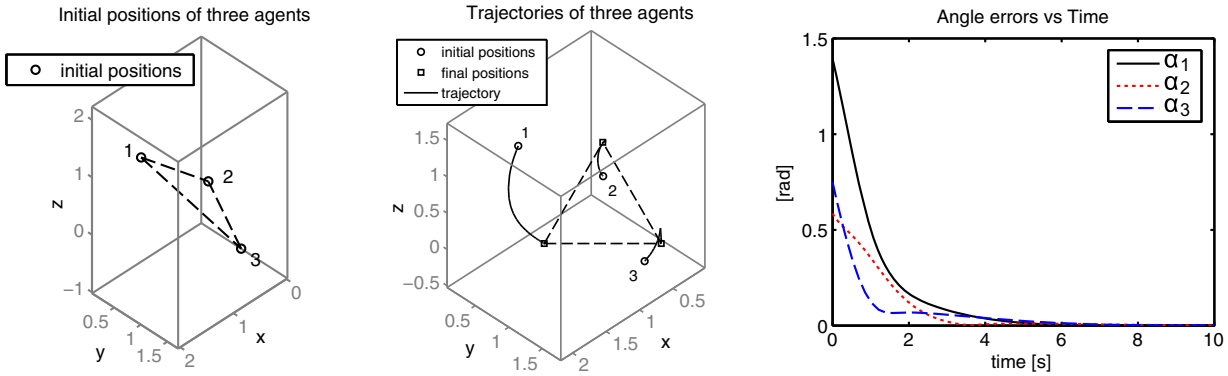

(A) The initial formation. (B) Trajectories and final formation. (C) The angles α_i vs. time [s].

FIGURE 19 Three agents form an equilateral triangle formation under the bearing-only cyclic pursuit control law (9) [Colour figure can be viewed at wileyonlinelibrary.com]

5.3 | Simulation 3: A three-agent formation in $\mathbb{R}^3$

We simulate a 3-agent formation in $\mathbb{R}^3$. The desired formation is an equilateral triangle whose desired bearing vectors are given by $\mathbf{g}_1^* = [-\sqrt{2}/2, 0, \sqrt{2}/2]^T, \mathbf{g}_2^* = [0, \sqrt{2}/2, -\sqrt{2}/2]^T$, and $\mathbf{g}_3^* = [\sqrt{2}/2, -\sqrt{2}/2, 0]^T$.

Simulation results are shown in Figure 19. The initial positions of the 3 agents are not parallel to the plane specified by the desired bearing vectors. The initial angle errors satisfy the condition $0 \leq \alpha_i \leq \frac{\pi}{2}, \forall i$. From the agents' trajectories depicted in Figure 19B, we observe that 3 agents asymptotically reach the desired plane and achieve the desired formation shape. Thus, we conclude that the simulation result is consistent with our analysis in Section 4.

6 | CONCLUSIONS

In this paper, a bearing-only formation control problem with directed cycle sensing topology has been studied in $\mathbb{R}^2$. We first derived necessary and sufficient conditions for the feasibility of planar formations defined by a set of desired bearing vectors. Then, we provided some results pertaining to the local asymptotic stability of the desired formation and instability of the undesired one for 3- and n-agent formations. Furthermore, an extended analysis of the 3-agent case in $\mathbb{R}^3$ was also presented. The stability analysis of the 3-agent formations in $\mathbb{R}^3$ illustrates the challenges involved in extending the results to higher dimensional spaces.

For future works, we aim to implement the formation control strategy proposed in this paper in quadcopter systems. To this end, collision avoidance between agents should be considered. Preventing collision separately, using vision-based techniques, is a challenging problem for the realization of the formation control law proposed in this paper. Another research direction could proceed along obtaining feasibility conditions for formations in higher dimensional spaces. Finally, it is hoped that the findings in this paper will lead to further results on bearing-only formation control over more general directed graphs.

ACKNOWLEDGEMENTS

The work of M. H. Trinh and H.-S. Ahn was supported by the National Research Foundation of Korea under grant NRF-2017R1A2B3007034.

The work of D. Mukherjee and D. Zelazo was supported in part at Technion-Israel Institute of Technology through a fellowship of the Israel Council for Higher Education and the Israel Science Foundation (grant 1490/1).

ORCID

Minh Hoang Trinh http://orcid.org/0000-0001-5736-6693
Dwaipayan Mukherjee https://orcid.org/0000-0001-6993-9305

Daniel Zelazo http://orcid.org/0000-0002-2931-245X
Hyo-Sung Ahn http://orcid.org/0000-0002-7939-0093

REFERENCES

1. Hendrickx JM, Anderson BDO, Delvenne JC, Blondel VD. Directed graphs for the analysis of rigidity and persistence in autonomous agent systems. *Int J Robust Nonlin Control*. 2007;17:960-981.
2. Krick L, Broucke L, Francis B. Stabilization of infinitesimally rigid formations of multi-robot networks. *Int J Control*. 2009;82(3):423-439.
3. Cao M, Morse AS, Yu C, Anderson BDO, Dasgupta S. Maintaining a directed, triangular formation of mobile autonomous agents. *Commun Inf Syst*. 2011;11(1):1-16.
4. Oh KK, Ahn HS. Formation control of mobile agents based on inter-agent distance dynamics. *Automatica*. 2011;47:2306-2312.
5. Sun Z, Mou S, Anderson BDO, Cao M. Exponential stability for formation control systems with generalized controllers: a unified approach. *Syst Control Lett*. 2016;93(5):50-57.
6. Oh KK, Park MC, Ahn HS. A survey of multi-agent formation control. *Automatica*. 2015;53:424-440.
7. Bishop AN, Basiri M. Bearing-only triangular formation control on the plane and the sphere. Paper presented at: 18th Mediterranean Conference on Control and Automation; 2010; Marrakesh, Morocco.
8. Bishop AN, Shames I, Anderson BDO. Stabilization of rigid formations with direction-only constraints. Paper presented at: Proceedings of the 50th Conference on Decision and Control (CDC) & European Control Conference (ECC); 2011; Orlando, FL.
9. Schoof E, Chapman A, Mesbahi M. Bearing-compass formation control: a human-swarm interaction perspective. Paper presented at: Proceedings of the American Control Conference; 2014; Portland, OR.
10. Bishop AN, Deghat M, Anderson B, Hong Y. Distributed formation control with relaxed motion requirements. *Int J Robust Nonlin Control*. 2015;25(17):3210-3230.
11. Trinh MH, Ko GH, Pham VH, Oh KK, Ahn HS. Guidance using bearing-only measurements with three beacons in the plane. *Control Eng Pract*. 2016;51:81-91.
12. Basiri M, Bishop AN, Jensfelt P. Distributed control of triangular formations with angle-only constraints. *Syst Control Lett*. 2010;59(2):147-154.
13. Zhao S, Lin F, Peng K, Chen BM, Lee TH. Distributed control of angle-constrained cyclic formations using bearing-only measurements. *Syst Control Lett*. 2014;63:12-24.
14. Zhao S, Zelazo D. Bearing rigidity and almost global bearing-only formation stabilization. *IEEE Trans Autom Control*. 2015;61(5):1255-1268.
15. Zelazo D, Giordano PR, Franchi A. Bearing-only formation control using an SE(2) rigidity theory. Paper presented at: Proceedings of the 54th IEEE Conference on Decision Control; 2015; Osaka, Japan.
16. Schiano F, Franchi A, Zelazo D, Giordano PR. A rigidity-based decentralized bearing formation controller for groups of quadrotor UAVs. Paper presented at: Proceedings of the 2016 IEEE/RSJ International Conference on Intelligent Robots Systems (IROS 2016); 2016; Daejeon, Korea.
17. Michieletto G, Cenedese A, Franchi A. Bearing rigidity theory in SE(3). Paper presented at: Proceedings of the 55th IEEE Conference on Decision and Control; 2016; Las Vegas, USA.
18. Eren T. Formation shape control based on bearing rigidity. *Int J Control*. 2012;85(9):1361-1379.
19. Trinh MH, Oh KK. Angle-based control of directed acyclic formations with three-leaders. Paper presented at: Proceedings of the 2014 IEEE International Conference on Mechatronics Control (ICMC); 2014; Jinzhou, China.
20. Trinh MH, Oh KK, Jeong KM, Ahn HS. Bearing-only control of leader first follower formations. Paper presented at: Proceedings of the 14th IFAC Symposium on Large Scale Complex Systems: Theory & Application; 2016; Riverside, CA.
21. Zhao S, Zelazo D. Bearing-based formation stabilization with directed interaction topologies. Paper presented at: Proceedings of the 54th IEEE Conference on Decision and Control; 2015; Osaka, Japan.
22. Zhao S, Zelazo D. Translational and scaling formation maneuver control via a bearing-based approach. *IEEE Trans Control Netw Syst*. 2015;PP(99):1-10. early access.
23. Mukherjee D, Trinh MH, Zelazo D, Ahn HS. Bearing-only cyclic pursuit in 2-D for capture of moving target. Paper presented at: 57th Israel Annual Conference on Aerospace Sciences; 2017; Israel.
24. Trinh MH, Mukherjee D, Zelazo D, Ahn HS. Planar bearing-only cyclic pursuit for target capture. Paper presented at: Proceedings of the 19th IFAC World Congress; 2017; Toulouse, France.
25. Marshall JA, Broucke ME, Francis BA. Formations of vehicles in cyclic pursuit. *IEEE Trans Autom Control*. 2004;49(11):1963-1974.
26. Mukherjee D, Zelazo D. Robustness of heterogeneous cyclic pursuit. Paper presented at: Proceedings of the 56th Israel Annual Conference on Aerospace Sciences; IEEE; 2016; Tel Aviv and Haifa, Israel.
27. Mukherjee D, Ghose D. Generalization of deviated linear cyclic pursuit. Paper presented at: Proceedings of the American Control Conference; IEEE; 2013; Washington DC, USA.
28. Mukherjee D, Ghose D. Deviated linear cyclic pursuit. *Proc R Soc A*. 2015;471(2184):20150682.
29. Park MC, Ahn HS. Stabilisation of directed cycle formations and application to two-wheeled mobile robots. *IET Control Theory Appl*. 2015;9:1338-1346.

30. Fathian K, Rachinskii DI, Summers TH, Gans NR. Distributed control of cyclic formations with local relative position measurements. Paper presented at: Proceedings of the 46th IEEE Conference on Decision and Control; 2016; Las Vegas, NV.
31. Eren T, Whiteley W, Belhumeur PN. Using angle of arrival (bearing) information in network localization. Paper presented at: Proceedings of the 45th IEEE Conference on Decision and Control; 2006; San Diego, CA.
32. Tron R, Carlone L, Dellaert F, Daniilidis K. Rigid components identification and rigidity control in bearing-only localization using the graph cycle basis. Paper presented at: Proceedings of the American Control Conference; IEEE; 2015; Chicago, USA.
33. Zhao S, Zelazo D. Localizability and distributed protocols for bearing-based network localization in arbitrary dimensions. *Automatica*. 2016;69:334-341.
34. Mesbahi M, Egerstedt M. *Graph Theoretic Methods in Multiagent Networks*. Princeton, NJ: Princeton University Press; 2010.
35. Loizou SG, Kumar V. Biologically inspired bearing-only navigation and tracking. Paper presented at: Proceedings of the 46th IEEE Conference on Decision and Control; 2007; New Orleans, LA.
36. Oh KK, Ahn HS. Formation control and network localization via orientation alignment. *IEEE Trans Autom Control*. 2014;59(2):540-545.
37. Montijano E, Cristofalo E, Zhou D, Schwager M, Sagues C. Vision-based distributed formation control without an external positioning system. *IEEE Trans Robot*. 2016;32(2):339-351.
38. Mori T. First results in detecting and avoiding frontal obstacles from a monocular camera for micro unmanned aerial vehicles. Paper presented at: Proceedings of the 2013 IEEE International Conference on Robotics and Automation (ICRA); 2013; Karlsruhe, Germany.
39. Horn RA, Johnson CR. *Matrix Analysis*. Cambridge, United Kingdom: Cambridge University Press; 2012.
40. Shevitz D, Paden B. Lyapunov stability theory of nonsmooth systems. *IEEE Trans Autom Control*. 1994;39(9):1910-1914.
41. Zhao S, Sun Z, Zelazo D, Trinh MH, Ahn HS. Laman graphs are generically bearing rigid in arbitrary dimensions. Preprint: https://arxiv.org/pdf/1703.04035.pdf.

How to cite this article: Trinh MH, Mukherjee D, Zelazo D, Ahn H-S. Formations on directed cycles with bearing-only measurements. *Int J Robust Nonlinear Control*. 2018;28:1074–1096. https://doi.org/10.1002/rnc.3921